

# FRAZIL AND ANCHOR ICE

## A MONOGRAPH

by

Gee Tsang. Ph. D., P. Eng.



NATIONAL RESEARCH COUNCIL OF CANADA  
ASSOCIATE COMMITTEE ON HYDROLOGY  
SUBCOMMITTEE ON HYDRAULICS OF ICE COVERED RIVERS

# FRAZIL AND ANCHOR ICE

## A MONOGRAPH

by

Gee Tsang. Ph.D., P. Eng.

NATIONAL WATER RESEARCH INSTITUTE  
CANADA CENTRE FOR INLAND WATERS  
FEBRUARY, 1982

PUBLISHED UNDER THE AUSPICES OF :  
NRC SUBCOMMITTEE ON HYDRAULICS OF ICE COVERED RIVERS.  
OTTAWA, ONT. CANADA

Available through prepaid orders only from:

Publications, NRCC/CNRC  
Ottawa, Canada K1A 0R6

## FOREWORD

In regions having long and severe winters, knowledge of frazil phenomena in rivers and lakes is critical for purposes of flow control, operation of hydraulic works, and estimation of the conveyance capacity of channels.

Despite the importance of these phenomena, previous scientific and engineering contributions on the subject have been fragmentary. Dr. Tsang's monograph on frazil ice is an admirable consolidation and presentation of currently available information on the subject, and should help considerably in making available in one volume this information.

The monograph is being published under the auspices of the NRC Subcommittee on Hydraulics of Ice Covered Rivers of which the author has been an active member for many years. The subcommittee is affiliated with the NRC Associate Committee on Hydrology. It is the hope of this subcommittee that the monograph will prove valuable to scientists and engineers working with frazil phenomena and that it will also set the stage for further advances through research.

K. S. Davar

Chairman of NRC Subcommittee  
on Hydraulics Of Ice Covered Rivers  
January 1982





## PREFACE

In 1979, I was asked by Prof. Bernard Michel, a well-known pioneer in ice research to write a section on frazil and anchor ice in nature for the contemplated book "River and Lake Ice Engineering" to be published by the International Association for Hydraulic Research (IAHR) in the near future. As I began the task, I was more and more aware of the acute shortage of a text book on the subject of frazil and anchor ice. Frazil and anchor ice can greatly affect the hydraulic behaviour of rivers and lakes but their discussions have been virtually excluded from nearly all the standard text books on hydraulics and limnology. I was convinced there is the need for a comprehensive, self-contained monograph devoted to such a topic for practising engineers and research scientists alike. Thus, I expanded the IAHR effort and wrote this monograph. I hope that periodic revision of this monograph would perpetuate its usefulness for workers in the field.

Although the first draft of the monograph was completed in 1980, because of my other commitments, it was not revised to its final form until now. I wish to thank my colleagues in the field, Prof. Bernard Michel of Laval University, Dean Thomas O'D. Hanley of Campion College, University of Regina, Dr. Spyros Beltaos of National Water Research Institute, Messrs. Thomas E. Wigle and Robert S. Arden of Ontario Hydro and Dr. Sylvester Petryk of Rousseau, Sauve, Warren Inc. for reviewing the first draft of the manuscript and their valuable comments. Their comments have been taken into consideration when the first draft was revised into the final version. I also wish to acknowledge the use of many photographs and charts from the quoted sources, both published and unpublished. Without these materials, this monograph could not be written. Finally, I wish to thank Drs. T. M. Dick and Y. L. Lau of National Water Research Institute for reading the final manuscript and giving approval for the publication of this monograph. The final manuscript was also read by colleagues of the NRC Subcommittee on Hydraulics of Ice-Covered Rivers, under its auspices this monograph is published.

The author

January 1982

## TABLE OF CONTENTS

	<u>Page</u>
<b>PREFACE</b>	i
<b>1.0 INTRODUCTION</b>	1
<b>2.0 NUCLEATION OF FRAZIL</b>	3
2.1 Requirement of Nuclei	3
2.2 Homogeneous Nucleation	3
2.3 Heterogeneous Nucleation	4
2.4 Theories of Nucleation of Frazil	4
2.5 Temperature of Frazil Producing Water	6
<b>3.0 THERMAL CONDITIONS FOR FRAZIL PRODUCTION</b>	9
3.1 General Governing Equation for Production and Transportation of Frazil	9
3.2 Heat Exchange at the Water Surface	12
3.2.1 Short wave radiation heat flux $q_1$	12
3.2.2 Long wave radiation heat flux $q_2$	15
3.2.3 Evaporative heat flux $q_3$ and convective heat flux $q_4$	18
3.2.4 Heat flux as a consequence of precipitation $q_5$	21
3.3 Heat Flux at River or Lake Bed	24
3.4 Conclusions: Hydrometeorological Conditions Conducive to Production of Frazil	25
3.5 Field Example	25
3.6 Thermal Conditions During the Formation of Frazil	28
<b>4.0 METAMORPHOSIS, GROWTH AND EVOLUTION OF FRAZIL</b>	33
4.1 Basic Shapes of Frazil Crystals	33
4.2 Formation and the Basic Forms of Flake Ice	35
4.3 Evolution of Frazil, from Crystals to Floes	37
4.4 Evolution of Frazil in Niagara River: A Field Example	44
<b>5.0 ACCUMULATION, TRANSPORTATION AND DEPOSITION OF FRAZIL IN RIVERS</b>	48
5.1 Accumulation of Frazil in the Form of River Ice Cover	48

	<u>Page</u>
5.2 Transport and Deposition of Frazil Under Ice Cover	50
5.3 Hanging Dams	52
5.3.1 Hanging dam and the factors controlling its growth and formation	52
5.3.2 Example of hanging dam formed in a river	53
5.3.3 Formation of hanging dam in river mouth	55
5.3.4 Formation of hanging dam in local deepenings or enlargements	56
5.3.5 Morphological changes of frazil in a hanging dam	56
5.3.6 Density and strength of hanging dam	56
5.3.7 Hardening and tunnelling of frazil accumulation	62
5.4 Effect of Frazil Presence to Velocity Distribution and Frazil Deposition	62
<b>6.0 ANCHOR ICE</b>	<b>64</b>
6.1 Turbulence and Its Effects on Cooling of Water and Formation of Frazil	64
6.1.1 Theory on turbulent diffusion of matters and properties	64
6.1.2 Turbulent transport of chilled water in lakes and rivers and its effect on frazil formation	65
6.1.3 Effect of stratification on turbulent diffusion and frazil formation	67
6.2 Formation of Anchor Ice	68
6.2.1 Anchor ice formed by underwater nucleation	68
6.2.2 Anchor ice formed by frazil adhesion	69
6.2.3 Formation of anchor ice and bottom material	71
6.3 Formation of Anchor Ice in Nature	72
6.4 Release of Anchor Ice from River Bottom	74
6.5 Formation of Anchor Ice in Sea Water	76
<b>7.0 TRANSPORT OF SEDIMENT AND RESISTANCE EFFECTS OF     FRAZIL AND ANCHOR ICE</b>	<b>78</b>
7.1 Transport of Sediment by Frazil and Anchor Ice	78
7.2 Resistance Effect of Frazil and Anchor Ice	80
7.3 Resistance Effect of Hanging Dams	82



	<u>Page</u>
8.0 CLOSURE	84
REFERENCES	86
APPENDIX Tables of Conversion	A1

## 1.0 INTRODUCTION

For quiescent water, supercooling and ice formation take place on the surface. The ice so formed is known as static ice. The static ice grows into an ice cover over the water surface.

For turbulent water, the turbulent mixing of the water results in a thick supercooled layer in which ice may form. The turbulence also suppresses the surface ice growth by breaking up the surface ice crystals and bringing them down to lower layers before they have a chance to grow. The ice formed in the turbulent, supercooled layer is in the form of countless small particles and is known as frazil. Frazil is also known as dynamic ice because of the dynamic process by which it is produced. According to Kivisild (1970), frazil is defined as:

"Fine spicules, plates or discoids of ice suspended in water. In rivers and lakes, it is formed in supercooled, turbulent water."

Under certain conditions, frazil may stick to underwater objects and produce what is known as anchor ice. Anchor ice may also be formed by direct nucleation of the supercooled water over the underwater objects. Both frazil and anchor ice are not at a stable state, but undergo continuous morphological changes.

In a river, the turbulence is produced by the flow. The relationship governing the degree of turbulence and the formation of frazil ice so far has not been systematically reported in the published literature. Based on field experience, Carstens (1970) considered that for rivers with a depth ranging from 1 to 5 m under windless conditions, a surface velocity of 0.6 m/s is required to prevent the formation of a surface ice cover and permit the formation of frazil. Under windy conditions, this critical surface velocity is reduced. Since in a river the turbulence is largely determined by the flow Reynolds number and the relative roughness of the channel, these two parameters probably should be considered as the most influential factors in determining the formation of frazil in a river, and not the surface velocity of the flow alone. Also, for the same Reynolds number and relative roughness, the turbulence level in the flow is affected by the stability condition of the flow. The stability parameter, which specifies the distribution of density with depth, therefore, should also be another important parameter in determining the turbulence condition, and consequently the formation of frazil in the flow.

In lakes, the turbulence is generated by surface agitation, mostly by wind shear. So far, no criterion has been established in the published literature, even an empirical one, identifying the hydrometeorological conditions under which frazil may form.

In this monograph, the nucleation of frazil, the thermal conditions under which frazil may be produced, the metamorphosis and evolution of frazil, the transportation of frazil under ice cover and the formation and properties of hanging dams, the formation and properties of anchor ice, the transport of sediment by frazil and anchor ice and the resistance effects of frazil and anchor ice will be discussed. It is hoped that this monograph will give its readers a complete and comprehensive understanding of frazil and anchor ice, their behaviours and hydrodynamic effects. Periodic revision and expansion of the monograph should give a state of the art text to practising engineers who are interested in the subject.

## 2.0 NUCLEATION OF FRAZIL

### 2.1 Requirement of Nuclei

As water changes its phase from liquid to solid, the latent heat of fusion is liberated. However, energy is absorbed to overcome the interfacial tension of the newly created ice/water interface. The latent heat of fusion liberated is proportional to the volume of the ice particle and the energy to overcome the interfacial tension of the ice/water interface is proportional to the surface area of the ice particle. In mathematical terms, one may write

$$\text{Liberated energy} \propto L^3$$

and

$$\text{Absorbed energy} \propto L^2$$

where  $L$  is a characteristic dimension of the ice particle. For an ice particle to grow, the body energy liberated has to be greater than the surface energy absorbed.

It is seen from the above expressions that for a small  $L$ , the body energy will be a higher order infinitesimal. This means that an ice particle cannot be formed or continue to grow unless a certain initial size has already been attained. This leads to the requirement of the presence of nuclei of a size larger than the minimum critical value upon which ice can nucleate and continue to grow.

### 2.2 Homogeneous Nucleation

The initial nuclei may come from the water itself. As the molecules of water move about, there are statistical chances by which some of the molecules will come to the geometric arrangements of ice crystals. Should the aggregate of molecules, or the embryo as it is often called, reach the critical size while the water is at or below the freezing temperature, continued growth of the embryo is possible and ice is formed in the water. This way of ice nucleation is known as homogeneous nucleation. The statistical chance of viable embryo formation increases with the degree of supercooling of the water, and only becomes significant when supercooling reaches as much as  $-40^{\circ}\text{C}$ . As such a

high degree of supercooling rarely happens in nature except in cases such as very high clouds, frazil formation by homogeneous nucleation in natural rivers and lakes can only be negligible.

### 2.3 Heterogeneous Nucleation

When organic or inorganic particles are present in the water, because of the interfacial tension force field at the surface, the statistical chance that the water molecules around the particles will obtain the geometric arrangement of ice is increased. For different materials of the particles, the enhancement of the statistical chances is different. As in the case of homogeneous nucleation, the chance of the water molecules around the solid particles obtaining the geometric arrangement of ice increases with the degree of supercooling. The nucleation of ice on foreign particles is known as heterogeneous nucleation. For particles of a given material, there exists a temperature below freezing that is known as the threshold temperature. Only when the water is supercooled to a temperature below the threshold temperature, will heterogeneous nucleation take place. For most inorganic materials, the threshold temperature falls between  $-4^{\circ}\text{C}$  to  $-30^{\circ}\text{C}$ . The highest threshold temperature is that of silver iodide of  $-3.5^{\circ}\text{C}$ . The threshold temperature of organic materials is generally higher than that of inorganic materials. The threshold temperature for withered leaves has been found to be as high as  $-1.3^{\circ}\text{C}$  and this temperature is considered as the highest temperature that heterogeneous nucleation can take place in water. As in natural waters organic and inorganic particles abound, there is no question on the availability of nuclei for heterogeneous nucleation. Heterogeneous nucleation of ice was known many years ago (Altberg, 1938).

In rivers and lakes, heterogeneous nucleation first occurs at the banks, where, because of the fluctuation of the water level, the bank is subject to periodic cooling by the air. When the bank is cooled to a temperature below the threshold temperature of the bank material, ice will nucleate on the bank. This way of heterogeneous ice nucleation in fact is the major mechanism for the formation of border ice.

### 2.4 Theories of Nucleation of Frazil

Some earlier researchers (Altberg 1936, Devik 1944) proposed that spontaneous heterogeneous nucleation accounts for the production of frazil in rivers and lakes. Their theory is now refuted by the fact that in natural rivers

and lakes, when frazil ice is being produced, the temperature of the water is seldom more than  $0.1^{\circ}\text{C}$  below the freezing point, well above the threshold temperature of all known materials. Hanley (1978) showed that at such a small supercool only ice particles are capable of nucleating frazil.

To circumnavigate the above weakness, Michel (1967) suggested that on the water surface, there exists a very thin layer of highly supercooled water where spontaneous heterogeneous nucleation takes place. Once ice crystals are formed in this thin layer, they are transported to the lower layers by turbulence to provide nuclei for further production of frazil. This proposal, which seemed to be acceptable for a while, is now subject to dispute because recent measurements of the surface temperature of water (Osterkamp 1975) showed that the surface temperature was well above the highest known threshold temperature when frazil ice was being produced in a stream. This dispute, however, was refuted by Michel (1980, personal communication) who pointed out that because the temperature measurement was made when frazil was already in the water, it did not prove that before the appearance of frazil the surface water had not been cooled to a subthreshold temperature.

The existence of a thin, supercooled layer on the surface is not really necessary for heterogeneous nucleation of frazil on the water surface. It is well known that in the atmosphere there are always plenty of dust particles. It is proposed here that in cold air these particles can be easily cooled to a subthreshold temperature. When some of the particles fall into the water, heterogeneous nucleation will occur because the water in immediate contact with these particles will be cooled down to a temperature below the threshold temperature. Since the air-borne dust particles are small and have small heat capacities, their temperature will quickly reach that of the ambient water after they have fallen into it. The formation of frazil by heterogeneous nucleation, therefore, is necessarily confined to a thin surface layer.

As noted earlier, ice particles already in the water can serve as nuclei for further ice nucleation. The first ice particles in the water that serve as nuclei are known as primary ice nuclei. Primary ice nuclei can come from surface ice and border ice when they are broken up by the current and entrained into the flow. As shown earlier, they can also be the frazil crystals that have been formed on the water surface by heterogeneous nucleation. Snow and sleet, when they have fallen into the water, may also serve as primary ice nuclei.



Another source (Osterkamp 1975) is the frozen sprays that are solidified in the cold air and have subsequently fallen back into the water. Frozen sprays are formed when a multitude of small water droplets are thrown into the air as a consequence of wave breaking, splashing and bubble bursting. In the cold air, these droplets can easily be cooled to the subthreshold temperature for heterogeneous nucleation to occur. While some scientists consider frozen sprays as the most important source of primary ice nuclei, some dispute it arguing that, because the temperature boundary layer above the water surface is thick, so the water sprays will only be subjected to a mild temperature close to 0°C rather than the subthreshold temperature.

As frazil ice crystals grow and tumble in the turbulent water, they agglomerate as well as being broken up by turbulence and collision. The number of ice nuclei, thus, is multiplied (Altberg, 1938). The new ice nuclei are known as secondary ice nuclei.

Nucleation of ice on secondary ice nuclei is known as secondary nucleation, although some researchers broadly consider secondary nucleation as nucleation on all ice nuclei. Since the production of secondary ice nuclei is a chain action, secondary nucleation on secondary ice nuclei can be a very effective process and is the principal mechanism in producing frazil ice in lakes and rivers.

## 2.5 Temperature of Frazil Producing Water

For secondary nucleation, the water temperature has to be less than the "equilibrium" temperature. The equilibrium temperature really is the depression of the freezing temperature because of impurities in the water and pressure adjustments. It is only slightly less than 0°C and can be calculated from (Osterkamp 1978):

$$T_e = 1.000 \times 10^{-2} - 0.751 \times 10^{-2} P - 1.860 \sum c_j \quad ^\circ\text{C} \quad (1)$$

where P is the number of atmospheric pressures the water is under and  $c_j$  is the concentration of the jth ions from the dissolved impurities in the water in units of molality. For natural fresh water,  $T_e$  generally is only a fraction of a hundredth of a degree below 0°C. As long as the water temperature is less than  $T_e$  and ice nuclei are available, frazil should continue to form and ice crystals should continue to grow.

In Fig. 1 there are two idealized curves; the upper curve shows the cooling of water with time and the lower curve shows the production of frazil in the supercooled water. The symbol  $M_i$  for the lower curve is the mass of frazil produced in the water. It is seen from Fig. 1 that as the water is supercooled to below the equilibrium temperature  $T_e$ , at a certain nucleation temperature  $T_n$ , frazil begins to form. At first, the latent heat of fusion released by the frazil is insufficient to compensate for the heat loss from the water because of the small number of ice crystals and the consequently slow rate of frazil production. The water temperature, therefore, continues to decrease, although at a slower rate. At the point where the latent heat of fusion released is equal to the rate of heat loss to the air, the water no longer has a net heat loss and its temperature reaches the lowest point  $T_m$ . Thereafter, increased latent heat liberation (probably by reason of accelerated secondary frazil nucleation) leads to a slow

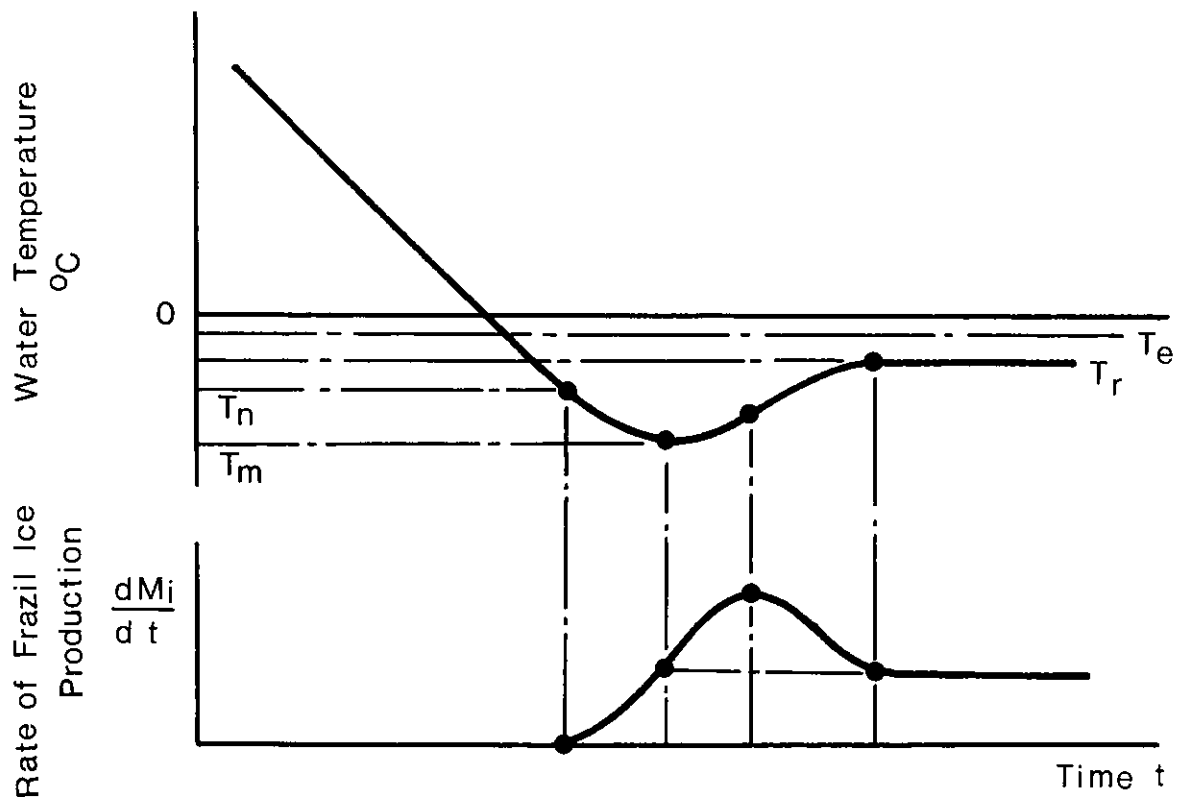


Fig. 1 Idealised curves for supercooling of water and production of frazil

increase of the water temperature until the residual temperature  $T_r$  is reached at which the rate of heat loss again is equal to the rate of latent heat liberation. It should be noted that the residual temperature is a variable depending on the hydrometeorological conditions under which frazil is formed. More will be said on this aspect later in the text.

The values of  $T_n$ ,  $T_m$  and  $T_r$  for natural rivers and lakes have not been well documented. Besides, as it can be seen from Fig. 1,  $T_n$  is very difficult to ascertain, especially under field conditions. From available data, however, they are found to be in the order of hundredths of a degree below  $0^{\circ}\text{C}$ .

The time scale from the onset of supercooling to the return of the temperature curve to the residual temperature depends on the rate of heat exchange, the heat capacity of the water body and the rate of production of frazil. Experiences show that for laboratory cases, if frazil is produced in a beaker, the time scale is measured in seconds. In a flume, the time scale is in minutes. For field cases, if frazil ice is generated in a small stream, the time scale is measured in tens of minutes and, in a large river, the time will be measured in hours. These time factors will give the engineers and scientists some comprehension of the speed of the frazil formation process. More will be said on the thermal balance of water for frazil and anchor ice production in the next chapter.

### 3.0 THERMAL CONDITIONS FOR FRAZIL PRODUCTION

#### 3.1 General Governing Equation for Production and Transportation of Frazil

For a control volume in frazil producing water, the following equation may be written for the conservation of heat:

$$\begin{aligned} \int_V \rho H_L \frac{\partial c_i}{\partial t} dV - \int_V c \rho \frac{\partial T}{\partial t} dV - \oint_A \hat{\vec{q}} \cdot \hat{\vec{n}} dA \\ + \oint_A \rho H_L (c_i \vec{v}) \cdot \hat{\vec{n}} dA - \oint_A c \rho (T \vec{v}) \cdot \hat{\vec{n}} dA = 0 \end{aligned} \quad (2)$$

where	V	=	the control volume
	A	=	the bounding surface of the control volume
	$\rho$	=	the density of water
	$H_L$	=	latent heat of fusion of ice
	$c_i$	=	concentration of frazil in water by weight
	c	=	specific heat of water
	T	=	temperature of water
	t	=	time
	$\vec{q}$	=	heat flux vector
	$\hat{\vec{n}}$	=	unit outward normal vector to the bounding surface
	$\vec{v}$	=	velocity vector relative to the bounding surface.

In the above equation, the first term is the rate of heat liberation in the volume because of the formation of frazil. The second term is the rate of heat absorption for increasing the temperature of the water in the volume. The third term is the net heat flux into the volume across the surface. The fourth term is the rate of heat left in the volume because of the outflux of frazil from the volume and the fifth term is the heat flux into the volume associated with the influx of water across the surface boundary. The above equation does not contain sink and source terms. However, they can be incorporated into the equation easily if the need arises to take care of situations such as waste heat input and the dumping of snow in a river, etc.

Strictly speaking, another term

$$-\frac{\partial}{\partial t} (\sigma A_f)$$

where  $\sigma$  is the interfacial tension between water and ice and  $A_f$  is the total surface area of all the frazil crystals, should also be added to the above equation to take into account the rate of heat absorbed to overcome the interfacial tension as the total ice surface is increased. However, this surface energy term is only important at the early stage of frazil nucleation and becomes progressively less important as the frazil crystals grow larger in size. This can be illustrated by comparing the total surface energy  $\sigma A_f$  of all the frazil crystals in  $1 \text{ m}^3$  of water at an exemplified concentration with the latent heat of fusion that is liberated by the frazil crystals. It was learnt from experiments that frazil crystal concentration in water can be as high as  $10^6/\text{m}^3$  and the maximum weight concentration of frazil in water can reach 0.5 percent when the crystals are in the suspended form (see 4.3). With the above concentrations and assuming a discoid shape for the frazil crystals with a diameter to thickness ratio of 20 (see 4.1), it can be calculated that the total surface area of all the crystals in  $1 \text{ m}^3$  of water comes to about  $45 \text{ m}^2$ . The interfacial tension between water and ice is approximately  $17 \times 10^{-3} \text{ J/m}^2$ . With this interfacial tension, the total surface energy of all the frazil crystals in  $1 \text{ m}^3$  of water can be calculated to be  $0.675 \text{ J}$ , which is small indeed compared to the latent heat of fusion of  $1.667 \times 10^6 \text{ J}$  liberated by 0.5 percent of frazil in the  $1 \text{ m}^3$  of water. Based on the above discussion, one sees that for all practical purposes, the surface energy term may be omitted from Eq. 2.

Using Gauss' theorem, Eq. 2 may be reduced to:

$$\int_V \left[ \rho H_L \frac{\partial c_i}{\partial t} - c \rho \frac{\partial T}{\partial t} - \nabla \cdot \vec{q} + \rho H_L \nabla \cdot (c_i \vec{v}) - c \rho \nabla \cdot (T \vec{v}) \right] dV = 0 \quad (3)$$

or

$$\rho H_L \left[ \frac{\partial c_i}{\partial t} + \nabla \cdot (c_i \vec{v}) \right] - \rho c \left[ \frac{\partial T}{\partial t} + \nabla \cdot (T \vec{v}) \right] - \nabla \cdot \vec{q} = 0 \quad (4)$$

which is the general differential equation governing the production of frazil.

As an example of using the above equations, one may study the case of a pond producing frazil during a windy day. If the whole pond is chosen as the control volume, then there will be no mass fluxes of frazil or water across the

boundary (assuming no groundwater inflow and no precipitation) and the last two terms in Eq. 2 will vanish and one obtains

$$\int_V \rho H_L \frac{\partial c_i}{\partial t} dV - \int_V c_p \frac{\partial T}{\partial t} dV - \oint_A \vec{q} \cdot \hat{n} dA = 0 \quad (5)$$

The above equation is also valid for a long stretch of a river. For such a control volume, the heat transfer associated with the mass fluxes of frazil and water at the two ends are insignificant in comparison to the other terms in Eq. 2.

Using average values, Eq. 5 may be rewritten as

$$\rho H_L \frac{\partial \bar{c}_i}{\partial t} V - \rho c \frac{\partial \bar{T}}{\partial t} V + \bar{q}_i A_b - \bar{q}_o A_s = 0 \quad (6)$$

where  $\bar{q}_o$  is the heat flux from the water to the air,  $q_i$  is the heat flux from the lake or river bed to the water,  $A_s$  and  $A_b$  are the area of the water surface and the lake or river bed respectively and the bar above the symbols means average values. For a wide lake or river,  $A_s$  and  $A_b$  are about the same so Eq. 6 can further be reduced to

$$\frac{\partial \bar{c}_i}{\partial t} = \frac{c}{H_L} \frac{\partial \bar{T}}{\partial t} + \frac{\bar{q}_o - \bar{q}_i}{\rho H_L \bar{D}} \quad (7)$$

where  $\bar{D}$  is the average depth of the lake or the river. Eq. 7 relates the heat fluxes to and from the water, the temperature of the water and the concentration of frazil in the control volume.

Immediately prior to the nucleation of frazil, the concentration of frazil in the control volume is zero, so  $\partial \bar{c}_i / \partial t$  is also zero and Eq. 7 is reduced to

$$\frac{\bar{q}_o - \bar{q}_i}{\rho H_L \bar{D}} = - \frac{c}{H_L} \left( \frac{\partial \bar{T}}{\partial t} \right)_n \quad (8)$$

where the subscript  $n$  indicates the time immediately before frazil begins to nucleate. If the weather conditions vary little from the onset of the period of frazil production, then the rate of heat loss from the control volume will remain the same and Eq. 8 may be substituted into Eq. 7 to give

$$\frac{\partial \bar{c}_i}{\partial t} = \frac{c}{H_L} \left[ \frac{\partial \bar{T}}{\partial t} - \left( \frac{\partial \bar{T}}{\partial t} \right)_n \right] \quad (9)$$



Integrating the above equation between  $t_n$ , the time of first frazil nucleation, and a later time  $t$ , one obtains

$$c_i = \frac{c}{H_L} (\bar{T} - \bar{T}_n) - \frac{c}{H_L} \left( \frac{\partial \bar{T}}{\partial t} \right)_n (t - t_n) \quad (10)$$

which is the equation for calculating the average frazil concentration in the control volume.

While the second term in the above equation increases with time, the first term varies within a small range only because of the small difference between  $T$  and  $T_n$  (see Fig. 1). Thus, if the time involved is sufficiently long, the average frazil concentration may be approximately calculated by the second term.

It is seen from Eq. 10 that the concentration of frazil in water is greatly affected by  $(\partial T / \partial t)_n$  and which, according to Eq. 8, is determined by the heat fluxes to and from the water body. It will be of interest to study the different heat flux components and to see which components are the most influential in the formation of frazil and anchor ice.

Although a change of thrust from ice physics to heat transfer at this point may appear to distract the readers from the main theme, this is considered necessary because in the past much concern has been centred around heat transfer in the study of frazil formation.

### 3.2 Heat Exchange at the Water Surface

The heat flux at the water surface  $q_0$  consists of the following components:

Short wave radiation  $q_1$

Long wave radiation  $q_2$

Evaporative heat transfer  $q_3$

Convective and conductive heat transfer  $q_4$  and

Heat transfer as a consequence of precipitation  $q_5$ .

In what follows, each component will be discussed. How each component may be evaluated will also be shown.

#### 3.2.1 Short Wave Radiation $q_1$

Short wave radiation comes mainly from the sun. The intensity of

solar energy reaching the outer surface of the earth is  $120 \text{ cal/cm}^2\text{hr}^*$  if the surface is normal to the sun ray and this amount is known as the solar constant. When reaching the earth's surface, however, the intensity of the solar radiation is less than the above amount because of atmospheric absorption and because in general the earth's surface is at an angle to the sun ray. Because the incident angle of the sun ray and the thickness of the atmospheric layer that the sun ray has to penetrate are both functions of the latitude of the locality, the intensity of the solar radiation reaching a point on the earth therefore is a function of the latitude of the point. The local topography also greatly affects the solar radiation intensity.

The effect of the incident angle and the atmospheric layer thickness on the intensity of solar radiation can be illustrated by the following example: At a sun angle of  $5^\circ$ , the water surface on the earth receives only  $0.6 \text{ cal/cm}^2\text{hr}$  direct sunshine. However, because of refraction and diffusion, eventually  $3.0 \text{ cal/cm}^2\text{hr}$  will fall onto the water surface if the sky is clear. For an overcast sky, the above value is reduced to  $1.0 \text{ cal/cm}^2\text{hr}$  (Devik, 1944).

It is seen from the above example that the solar radiation eventually reaching the earth's surface consists of the direct radiation and the indirect radiation, or the sky radiation, two parts. This combined radiation meteorologically is called "insolation" and may be denoted as  $q_1^*$ .

Insolation for a cloudless sky at different latitudes may be obtained from available meteorological tables (List, 1968; Tables 136, 152) and insolation under different cloud covered conditions may be calculated from the following equation:

$$q_1^* = q_{1c}^* (0.35 + 0.061 (10-C)) \quad (11)$$

where  $q_{1c}^*$  is the insolation under clear sky conditions and C is cloud coverage in tenths (ranging from 0 for a clear sky to 10 for a completely overcast sky).

A different empirical equation of the form of

$$q_1^* = q_{1c}^* (a - bC^m) \quad (12)$$

---

\* The  $\text{cal/cm}^2 \text{ hr}$  unit instead of the SI unit is used because most quoted figures from past experiments used in this monograph were in this unit.

was quoted by Carstens (1970), where a, b and m are coefficients depending on latitude and topography. The simplest equation of the above form is (Devik, 1931)

$$q_1^* = q_{1C}^* (1 - 0.09 C) \quad (13)$$

A plotting of the linear equations 11 and 13 on the same graph would show that while the two equations give close results when the cloud coverage is small, large differences occur when the cloud coverage is high. Such differences should be expected because both empirical equations ignore the characteristics of the cloud. According to List (1968),  $q_1^*$  not only is a function of C, but a function of the type of the cloud also. It should also be noted that Eq. 11 does not apply when  $C=0$  or close to it because at  $C=0$ , it gives  $q_1^*=0.96 q_{1C}^*$ , not  $q_1^*=q_{1C}^*$  as it should.

Of the solar heat flux  $q_1^*$  reaching the water surface, a fraction  $\alpha$  is reflected back into the space and only

$$q_1 = (1 - \alpha) q_1^* \quad (14)$$

is absorbed.  $\alpha$  is called the albedo of the water surface. According to Carstens (1970), the albedo of water surface only varies from 0.08 to 0.10. However, Dingman et al (1968) quoted water surface albedo values ranging from 0.05 to 0.30, being a strong function of solar altitude and also depending on cloud conditions.

It is seen from the above discussions that with the present state of knowledge, an accurate evaluation of the solar heat flux to a water surface is still difficult. There are many questions that still need to be settled. Coming back to the topic of frazil formation, one can see that solar radiation represents a positive heat flux to the water body. For promoting frazil formation in water, the solar heat flux to the water should be as small as possible. During the night, solar radiation is near zero. Therefore, other things being equal, frazil is more likely to form at night. On the other hand, solar radiation is a very important factor in warming up the water during the day. Whether frazil would form in the water or not, therefore, is to a large extent dependent on the heat stored in the water and consequently on the daytime solar heat influx.

### 3.2.2 Long Wave Radiation Heat Flux $q_2$

Like any surface that has a temperature greater than absolute zero, long wave radiation is emitted by the water surface. According to the Stefan-Boltzmann law, the heat flux emitted by the water surface is given by

$$q_{2w} = \epsilon \sigma T_w^4 \quad (15)$$

where  $\epsilon$  is the emissivity of the water surface and is equal to 0.97 (Anderson, 1954),  $\sigma$  is the Stefan-Boltzmann constant of  $4.879 \times 10^{-9} \text{ cal/cm}^2\text{hr}^\circ\text{K}^4$  and  $T_w$  is the water surface temperature in  $^\circ\text{K}$ . According to the above equation, it can be calculated that the long wave radiation heat flux emitted by a freezing water surface is  $26.28 \text{ cal/cm}^2\text{hr}$ .

The atmosphere, being a body with a temperature above absolute zero, also emits long wave radiation. This long wave radiation reaches the water surface and is partly absorbed and partly reflected back into the atmosphere. Since the emissivity of the water surface is 0.97, nearly unity, water can be approximately considered as a black body to long wave radiation. For a black body, the albedo is zero. Thus, all the long wave radiation emitted by the atmosphere may be approximately considered as having been absorbed by the water although actual measurements showed that about three percent of the long wave radiation is reflected.

When the sky is clear, the long wave radiation emitted by the atmosphere and reaching the water surface is given by (Anderson, 1954)

$$q_{2a} = (0.68 + 0.036 e_a) \sigma T_a^4 \quad \text{cal/cm}^2\text{hr} \quad (16)$$

where  $e_a$  is the vapour pressure of the atmosphere in millibars and  $T_a$  is the air temperature in  $^\circ\text{K}$ . It is seen from the above equation that the moister the air, the more heat will be emitted by long wave radiation.

When the sky is clear, part of the long wave radiation emitted by the water surface and by the atmosphere will go into the space. However, when the sky is cloud covered, the outgoing long wave radiation is reflected by the cloud back onto the earth. The reflected part of the long wave radiation emitted by the water surface goes into the heating of the atmosphere and that eventually

will lead to a warmer atmosphere and a more intense atmospheric long wave radiation. The part of the radiation that is emitted by the atmosphere and reflected by the cloud cover, will add to the long wave radiation received by the water surface. Warmer weather in the lower atmosphere because of cloud cover is commonly known as the "green house" effect.

The intensity of the long wave radiation that will reach the water surface under cloudy conditions may be calculated from the following empirical equation (Anderson, 1954):

$$q_{2a} = (a + b e_a) \sigma T_a^4 \quad \text{cal/cm}^2\text{hr} \quad (17)$$

with

$$a = 0.740 + 0.025C \exp(-1.92 \times 10^{-4} H) \quad (18)$$

and

$$b = 4.9 \times 10^{-3} - 5.4 \times 10^{-4} C \exp(-1.97 \times 10^{-4} H) \quad (19)$$

where H is the height of the cloud in metres above 500 m. For cloud height less than 500 m, H=500 is used. Again it should be noted that because of its empirical nature, Eq. 17 does not give exactly the same result when C=0 as that given by Eq. 16.

The net long wave radiation heat loss to the water body is the difference between the long wave radiation emitted by the water surface and the long wave radiation emitted by the atmosphere and absorbed by the water surface, or

$$q_2 = q_{2w} - q_{2a} \quad (20)$$

As  $q_{2w}$  is nearly constant, the variation of  $q_2$  is determined by the variation of  $q_{2a}$ . To favour frazil formation,  $q_2$  should be large or  $q_{2a}$  should be small. According to Eqs. 16 to 19, one sees that  $q_{2a}$  is small when the air temperature

$T_a$  is low, the vapour pressure  $e_a$  or the humidity of the air is low, the cloud coverage is low and the cloud ceiling is high, or, better still, there is no cloud cover at all. In conjunction with the conclusion that has been drawn in the earlier discussion on short wave radiation, one can say that a cold night with a clear sky and a low humidity air will favour the loss of heat from the water body and consequently the formation of frazil.

It is important to note the different ways of heating and cooling of water by short wave and long wave radiations. For short wave radiation or solar radiation, it can penetrate water to a great depth, its absorption by water therefore is gradual and this leads to the warming up of the whole water layer. For the remaining part of the radiation that reaches the bottom, part of it is absorbed by the bottom and part is reflected. While the reflected part will bounce back and forth between the bottom and the surface and eventually be absorbed by the water layer and the bottom (minus the small part that is reemitted back into the space), the absorbed part heats up the bottom which in turn warms up the water from below. Thus, the heating up of water by short wave radiation is effective for the whole water layer.

For long wave radiation, the situation is quite different. Long wave radiation can hardly penetrate a water layer more than a fraction of a millimetre without being mostly absorbed. Thus, the emission and absorption of long wave radiation are necessarily confined to a very thin surface layer and this can lead to intense chilling of the water surface. The formation of surface ice at night over a relatively warm water layer is not unusual especially when the turbulence level of the water is low.

The net long wave radiation from the water surface under conditions conducive to frazil and anchor ice formation has been measured by Devik (1944) in the field. The net long wave radiation heat flux obtained by him ranged from  $13.8 \text{ cal/cm}^2\text{hr}$  when the sky was clear to  $4.9 \text{ cal/cm}^2\text{hr}$  when the sky was cloud covered. In studying the formation of frazil in the Ottawa River, Williams (1972) found that the net long wave radiation varied between 7 to  $15 \text{ cal/cm}^2\text{hr}$ . The higher values occurred at nights with clear skies. He showed that when there was no wind, such long wave radiations could account for from 30 to 40 percent of the total heat loss of the river. Long wave radiation heat loss, therefore, is an important factor determining the formation of frazil and anchor ice in water.



In the above discussions, short wave radiation and long wave radiation are discussed separately. In practice, short wave and long wave radiations are measured together as total radiation heat flux by a radiometer. At night, as the short wave radiation becomes negligible, the total radiation is equal to the long wave radiation alone.

### 3.2.3 Evaporative Heat Flux $q_3$ and Convective and Conductive Heat Flux $q_4$

The evaporative heat loss and the convective and conductive heat loss will be discussed here together because the two processes are similar.

As the name implies, the convective and conductive heat flux  $q_4$  contains both the heat transferred by convection and the heat transferred by conduction. Under most practically important conditions, however, the conductive heat transfer is much smaller than the convective heat transfer.  $q_4$  thus may be considered as consisting of the convective heat flux alone.

The convective heat transfer between the water and the air depends on the temperature difference between the water and the air and the wind present. When there is no wind, the heat is transferred by the natural circulation that is set up by the temperature difference and this is known as natural convection. When there is a wind, the eddies in the flow field also help to transport the heat. The transfer of heat by the eddies in the turbulent wind shear field is known as forced convection. When the wind is strong, forced convection is the main transfer mechanism. When the wind is weak, natural convection is the predominant mode.

Under forced convection conditions, the evaporative heat transfer and the convective (sensible) heat transfer are governed by the following analogous diffusion equations:

$$q_3 = -K_E \rho_a H_{LE} \left( \frac{dE}{dz} \right) \quad (21)$$

and

$$q_4 = -K_c \rho_a c_a \left( \frac{dT}{dz} \right) \quad (22)$$

where  $E$  is the specific humidity (the ratio of the mass of water vapour to the mass of dry air in a given volume of mixture),  $z$  is the vertical direction,  $\rho_a$  is the density of the air,  $c_a$  is the specific heat of air under constant pressure,  $H_{LE}$  is the latent heat of evaporation of water and  $K_E$  and  $K_C$  are turbulent diffusion coefficients for vapour and sensible heat respectively. The ratio of  $q_4/q_3$  is known as the Bowen ratio and may be denoted as  $R$ .

If the transport mechanism of vapour is assumed to be the same as the transport mechanism of the air itself, an analogous assumption often used in the study of turbulent heat and mass transfer, then  $K_E$  and  $K_C$  will be equal and from Eqs. 21 and 22, when they are written between the water surface and the atmosphere and after appropriate conversion constants are substituted, one obtains (Dingman et al, 1968)

$$R = 6.1 \times 10^{-4} P \frac{T_w - T_a}{e_{sw} - e_a} \quad (23)$$

where  $P$  is the atmospheric pressure in millibars,  $e_{sw}$  is the saturated vapour pressure at  $T_w$ , also in millibars, and the other symbols and their units have been defined earlier. In studying the evaporative heat flux and the convective (sensible) heat flux, the general approach is to calculate  $q_3$  or  $q_4$  from one of the available empirical equations and then evaluate the other from the Bowen ratio.

It may be noted, however, that because of the analogous assumption used and the inherent restrictions that come with it, the Bowen ratio can be subject to some errors under certain meteorological conditions. Some researchers (Hanley, 1980, personal communication), therefore, advocate independent evaluation of  $q_3$  and  $q_4$ . In this monograph, however, the general approach of using the Bowen ratio is used because experimental measurements indicated that near the freezing temperature such an assumption would not lead to large errors.

There are many empirical equations for calculating the evaporative heat loss and here the one originally obtained by Kohler is presented (Dingman et al, 1968):

$$q_3 = (0.131 + 0.306 v_{a2}) (e_{sw} - e_{a2}) \text{ cal/cm}^2\text{hr} \quad (24)$$

where  $v_{a2}$  and  $e_{a2}$  are the wind velocity (m/s) and the vapour pressure (mb) at 2 m height respectively. The multiplication of Eqs. 23 and 24 and with the approximation that  $P=1000$  mb gives

$$q_4 = (0.080 + 0.186 v_{a2}) (T_w - T_a) \text{ cal/cm}^2\text{hr} \quad (25)$$

Based on field data, Rimsha and Donchenko (Rimsha and Donchenko, 1957; Dingman et al, 1968; List and Barrie, 1972) obtained the following equation for the sensible heat loss:

$$q_4 = \left[ (0.333 + 0.0146 (T_w - T_a)) + 0.1625 v_{a2} \right] (T_w - T_a) \text{ cal/cm}^2\text{hr} \quad (26)$$

Comparing Eqs. 25 and 26, one sees that the constant 0.080 in Kohler's equation is replaced by a coefficient depending on  $(T_w - T_a)$  in Rimsha and Donchenko's equation. Rimsha and Donchenko considered that this  $(T_w - T_a)$  depending coefficient takes into account the transfer of heat due to natural convection that has been ignored in the forced convection differential equations 21 and 22. From the above equation and Eq. 23, one obtains the following evaporative heat flux equation:

$$q_3 = \left[ 0.520 + 2.275 \times 10^2 (T_w - T_a) + 0.253 v_{a2} \right] (e_{sw} - e_a) \text{ cal/cm}^2\text{hr} \quad (27)$$

The plotting of the Kohler equations and the Rimsha and Donchenko equations on the same graph would show that there are differences, especially when the water and air temperature difference  $T_w - T_a$  is large. Since each set of empirical equations was derived under its own special conditions, it is difficult to say which set is superior. One can see, however, that the question of evaluating the evaporative heat flux and the convective sensible heat flux has still not been precisely answered and there are things yet to be settled.

Besides the above empirical equations, other empirical equation have also been reported, including those given by Devik (Carstens, 1970) and those given by Ferguson and Cork (1972).

It should be noted that in the above empirical equations, the direction of the wind is not considered as a parameter. This is disputable physically, as the boundary layer over the water surface will be better developed and the transport of heat and mass will be more effective if the wind blows along its axis than if the wind blows perpendicular to its axis. This is especially true for a slender water body.

The following figures were quoted by Devik (1944) based on his field measurements:

At an air temperature of  $-10^{\circ}\text{C}$  and a vapor pressure of 3.4 mb, the rates of heat loss were -

$$\text{At } v_{a2} = 0,$$

$$q_3 = 1.7 \text{ cal/cm}^2\text{hr}$$

$$q_4 = 2.8 \text{ cal/cm}^2\text{hr}$$

$$\text{At } v_{a2} = 5 \text{ m/s}$$

$$q_3 = 7.7 \text{ cal/cm}^2\text{hr}$$

$$q_4 = 11.5 \text{ cal/cm}^2\text{hr}$$

With the above weather parameters, the evaporation and convective heat fluxes calculated according to Rimsha and Donchenko's equations are:

$$\text{At } v_{a2} = 0$$

$$q_3 = 1.95 \text{ cal/cm}^2\text{hr}$$

$$q_4 = 4.79 \text{ cal/cm}^2\text{hr}$$

$$\text{At } V_{a2} = 5 \text{ m/s}$$

$$q_3 = 5.24 \text{ cal/cm}^2\text{hr}$$

$$q_4 = 12.92 \text{ cal/cm}^2\text{hr}$$

A comparison of the measured values with the calculated values will demonstrate the expected degree of accuracy of the empirical equations.

### 3.2.4 Heat Flux as a Consequence of Precipitation $q_5$

As snow falls into the water, heat is lost to warm the snow from the air temperature to the water temperature and to melt the snow. From the conservation of heat, the heat flux  $q_5$  for heating up and melting the snow is given by

$$q_5 = p_s \left[ H_L + c_s (T_w - T_s) \right] \quad (28)$$

where  $p_s$  is the rate of snowfall per unit area ( $\text{g}/\text{cm}^2\text{hr}$ ),  $H_L$  is the latent heat of fusion of ice,  $c_s$  is the specific heat of snow and  $T_s$  is the temperature of the snow.

Although precipitation has been identified as a component of the total heat transfer, it is not an important component during the time of frazil production because, according to the earlier discussion on long wave radiation heat loss, to promote frazil and anchor ice formation in water, a clear sky and a low humidity air are required. When the sky is clear and the humidity is low, it is implicit that there will be little precipitation.

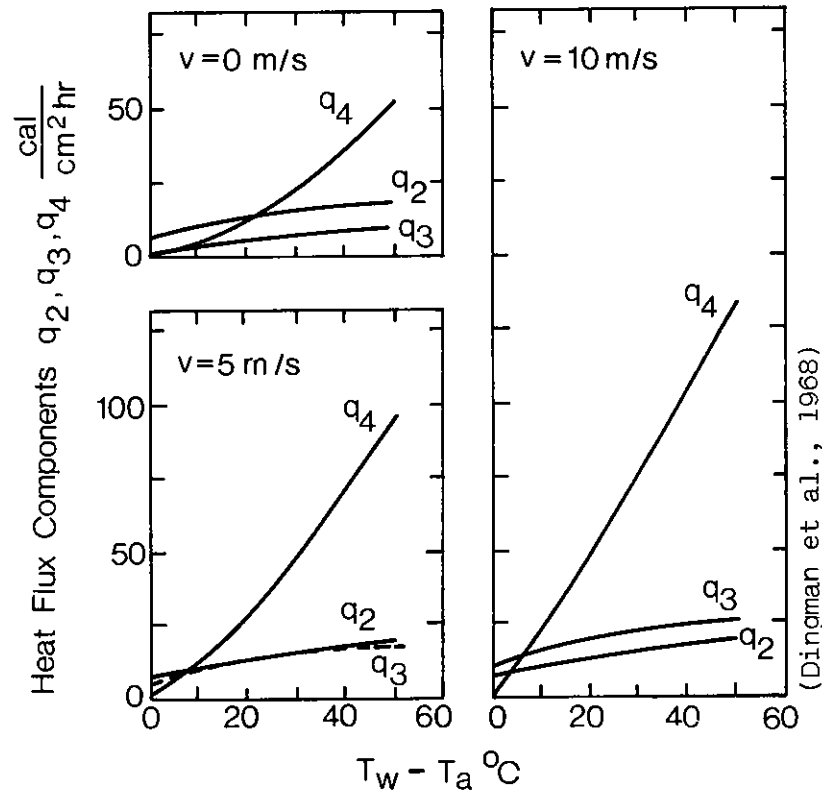


Fig. 2  $q_2$ ,  $q_3$  and  $q_4$  at different wind velocities and water-air temperature differences

Figure 2 is a plot showing the long wave radiation heat loss, the evaporative heat loss and the convective heat loss fluxes as functions of the wind velocity and the water and air temperature difference (Dingman et al, 1968). In plotting the curves, the sky was assumed clear and the relative humidity was assumed to be 50 percent. The Rimsha-Donchenko equations were used to calculate  $q_3$  and  $q_4$ . Although in Fig. 2 curves are plotted for  $T_w - T_a$  as large as  $60^\circ\text{C}$ , for most practically important cases where the formation of frazil ice and anchor ice is involved, the water and air temperature difference seldom exceeds  $30^\circ\text{C}$ . It is seen from Fig. 2 that when  $T_w - T_a$  is less than  $30^\circ\text{C}$ ,  $q_2$ ,  $q_3$  and  $q_4$  are all important. When the wind is low and the temperature difference is small, the long wave radiation heat flux is the most important. However, as the wind speed increases and the temperature of the atmosphere decreases, the convective sensitive heat flux becomes the most important heat loss term. The evaporative heat loss is less than the long wave radiation heat loss when the wind speed is less than 5 m/s. However, when the wind speed is increased to above 5 m/s, the evaporative heat loss becomes more important than the long wave radiation heat loss.

Table 1 (Asvall, 1972) gives the total heat loss rate at the water surface at different wind speeds, different cloud coverages and different air temperatures. The table was constructed based on measured data from Norway. In the table, the humidity effects have been absorbed in the figures when they were derived. In studying the formation of frazil ice in the Ottawa River, Williams (1972) also measured the total heat loss flux from the water surface. His measured values were within the range shown in the table. For his particular site, Williams found that frazil problems could be expected when the total heat loss flux from the river was greater than  $31 \text{ cal/cm}^2\text{hr}$ .

**TABLE 1 TOTAL HEAT LOSS RATES AT WATER SURFACE**

Cloud Coverage	Wind Speed	Heat Loss Rate (cal/cm <sup>2</sup> hr)			
		Air Temperature °C			
0-10	m/s	0	-10	-20	-30
0	1	11.9	24.1	34.6	45.4
	5	12.6	33.5	51.6	67.5
5	1	6.9	19.1	29.5	40.4
	5	7.6	28.9	46.5	62.4
10	1	2.2	14.1	24.8	35.6
	5	2.9	23.8	41.8	57.7

(Asvall, 1972)



### 3.3 Heat Fluxes at River or Lake Bed

The heat flux at the river or lake bed includes the following components:

Heat input associated with groundwater inflow  $q_6$

Geothermal heat input  $q_7$ , and

Heat generated because of bed friction or head loss  $q_8$ .

With reference to Eq. 2, one sees that the groundwater heat inflow can either be taken care of by the third term or by the fifth term of the equation although presently it is included in the third term as a boundary heat flux component. Both the groundwater heat input  $q_6$  and the geothermal heat input  $q_7$  are fairly constant heat fluxes and, generally speaking, are also quite small. Thus, in studying the formation of frazil and anchor ice in water, they are usually ignored.

As to the heat flux generated by bed friction or head drop, for a river of discharge  $Q$  ( $m^3/s$ ) descending a vertical drop of  $\Delta h$  (m), the rate of heat generated is given by

$$p = \frac{10^3}{427} Q \Delta h \quad \text{k cal/s} \quad (29)$$

where 427 converts the work in kgf-m to work in k cal. The division of the above power by the surface area  $wL$  of the river, where  $w$  is the width of the river (m) and  $L$  is the length of the reach (m) over which  $\Delta h$  takes place, gives the heat flux produced by bed friction or head loss that has to be dissipated by the river surface

$$q_8 = \frac{10^3}{427} \frac{Qs}{w} \text{ (kcal/m}^2\text{s)} = 843 Qs/w \text{ (cal/cm}^2\text{hr)} \quad (30)$$

where  $s = \Delta h/L$  is the slope of the river. It is seen from the above equation that  $q_8$  can be quite large if the rate of discharge is high, the slope of the river is steep and the river is narrow. This explains why in waterfalls and in fast rapids, ice often is not formed.

When the total heat loss flux of a river is greater than the total heat gain flux, the river will be cooled down and border ice will be formed from the banks and partially covering the river. However, as the river becomes partially

ice covered, the surface width  $w$  is reduced and this, according to Eq. 30, leads to a higher  $q_g$ . Therefore, for a fast flow, when the border ice grows to a certain point and the heat flux  $q_g$  (plus other heat influxes) becomes sufficiently large that it can no longer be completely dissipated by the water surface, the border ice will grow no more and the heat balance of the river at this point reaches the point of equilibrium. The above explains why, for fast rivers, a narrow opening is often observed in the ice cover.

For most natural rivers, the rate of discharge  $Q$ , the bed slope  $s$  and the river surface width  $w$  vary little during the time of frazil formation, so the heat flux generated by bed friction  $q_g$  is not a determining factor. However, for rivers downstream of control structures, the fluctuation of the discharge with time can be substantial and this, according to Eq. 30, can lead to quite different frazil conditions.

#### 3.4 Conclusions: Hydrometeorological Conditions Conducive to Production of Frazil

At this point, discussions on the thermal balance of water can be concluded. It is seen from the above discussions that to enhance the formation of frazil and anchor ice in water, a fast chill of the water to a supercooled temperature is required. Such a fast chill of the water requires zero solar radiation heat input, and large heat losses by long wave radiation, evaporation and convection from a small water body. In common language, one says that frazil ice and anchor ice are likely to form on a clear cold night when the wind is strong, the humidity of the air is low and the river is at the minimum flow, especially if such a night follows a cold, windy and cloudy day.

#### 3.5 Field Example

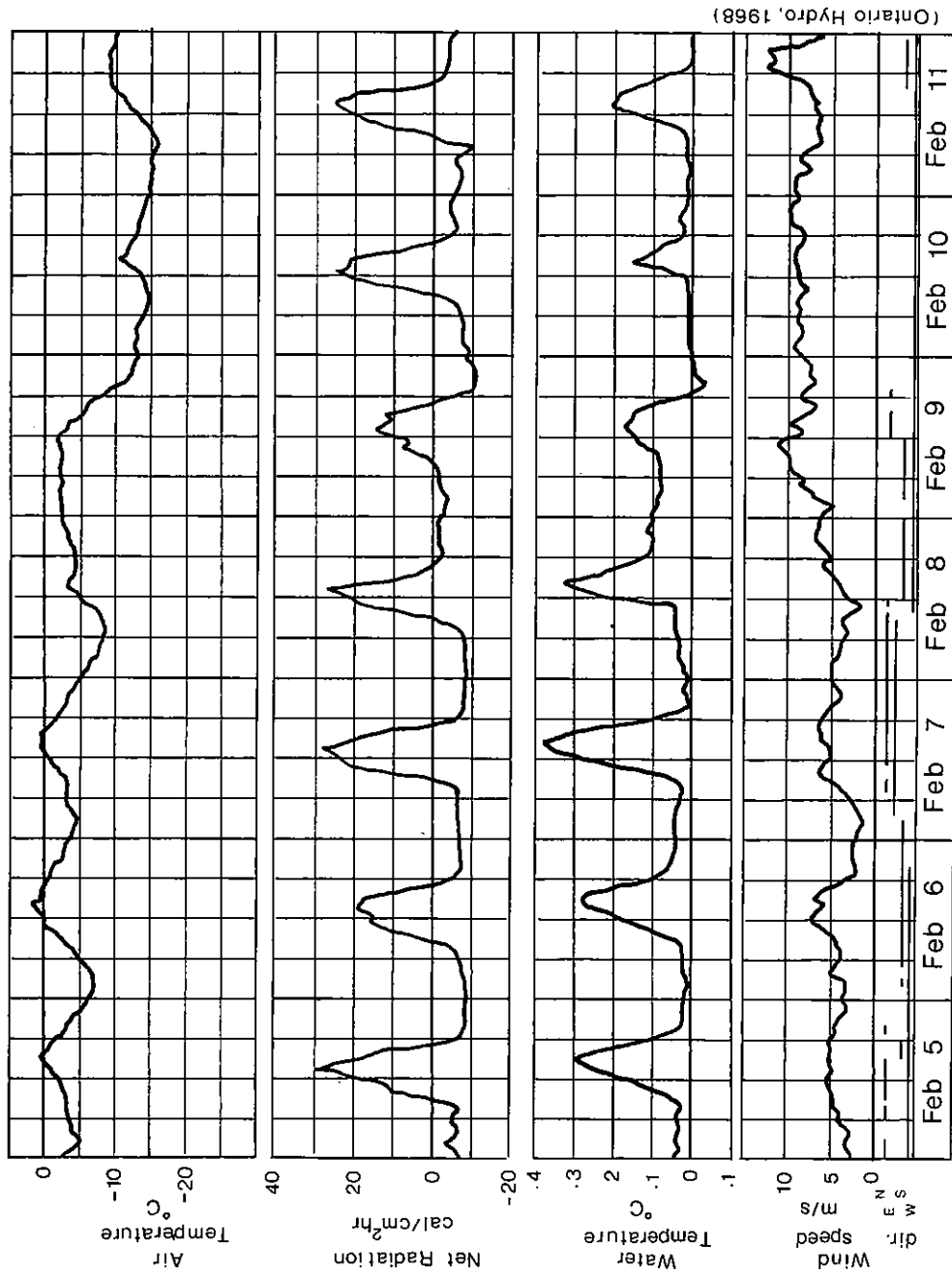
Fig. 3 is an example showing the cooling of the water in the Niagara River and the effect of the different important meteorological parameters (Ontario Hydro, 1968). In the diagram, recordings of the air temperature, the total radiation (short wave and long wave), the water temperature and the wind velocity are shown. It is seen from the radiation recording in Fig. 3 that the radiation heat flux to and from the water followed a strong diurnal pattern, indicating the strong effect of the solar radiation. During the day, there was a heating period during which the radiation heat flux increased from zero in the morning to the maximum value a little after noon. From that point on it began

to decrease and reached the zero value again sometime between 1600 to 1700 hr. The maximum radiation heat influx fell in the range of 15 to 30 cal/cm<sup>2</sup>hr, which may be considered as typical for southern Ontario. Different cloud cover conditions were responsible for the different peak radiation values. As the sun began to set, the long wave radiation emitted by the water surface began to surpass the solar radiation received by the water and the net radiation changed from positive to negative. It is seen from Fig. 3 that the long wave radiation heat loss during the night was rather constant, due to the nearly freezing temperature of the water. The long wave radiation heat flux at night varied between 1 to 12 cal/cm<sup>2</sup>hr, depending on the cloud coverage. The largest value of about 12 cal/cm<sup>2</sup>hr that occurred on February 9 was very close to the value given by Devik (1944) of 13.8 cal/cm<sup>2</sup>hr for long wave radiation when there is no greenhouse effect.

The water temperature recording shown in Fig. 3 follows closely the diurnal pattern of the radiation recording, indicating the strong effect of the radiation heat flux on the heating and cooling of the water. For February 9, because of the small heat reserve received during the day and the large long wave radiation during the night, the water became supercooled soon after sunset and frazil production (and anchor ice) was observed during the night.

It is seen from Fig. 3 that the diurnal variation pattern was also borne by the air temperature recording; one may conclude that radiation also greatly affected the air temperature which, in turn, affected the heat flux between the air and the water.

In discussing the convective heat loss, it was shown that the convective heat loss is increased when the wind velocity is increased and when the air temperature is decreased (see Eqs. 25 and 26). Such a relationship, indeed, is confirmed by Fig. 3. It is seen from Fig. 3 that the high wind speed and the low air temperature for February 10 and 11 have led to a low daytime temperature of the water for these two days in spite of the fact that the net radiation was above average. For the night of February 9, the low air temperature and the strong wind, plus a high long wave radiation, following a day of small heat gain led to the supercooling of the water and the subsequent formation of frazil and anchor ice in the river. A similar examination can also be made of the evaporative heat loss had the humidity data been recorded.



(Ontario Hydro, 1968)

FORT ERIE, NIAGARA RIVER, 1968.

Fig. 3 Weather recording during cooling of Niagara River

Field observations showed that only on February 9 was the water supercooled at night and frazil and anchor ice were formed. For the other nights, the nighttime cooling was insufficient to bring the water temperature to below freezing. However, even for these nights, ice platelets were observed to form on the surface. The formation of surface ice platelets was understandable because it was mentioned earlier that intense night time long wave radiation can cause intense chill to the surface layer where ice can be nucleated. It is seen from Fig. 3 that, for the several nights in question, the night time radiation was quite strong. According to Kivisild's definition of frazil shown in the Introduction, the surface ice platelets can also be broadly considered as a form of frazil.

### 3.6 Thermal Conditions During the Formation of Frazil

After studying the heat fluxes to and from the control volume which ultimately lead to supercooling of the water and the nucleation of frazil, it will be of interest to see how frazil is produced following its initiation.

The rate of increase of frazil in water is determined by the following three factors:

1. How many frazil crystals are there in the water?
2. How fast do these crystals grow?
3. How fast do these frazil crystals multiply?

The first factor is the result of historical events of the frazil producing water and thus is a function of time.

For the second factor, it depends on how fast heat can be removed from the ice crystals and thus is a function of the degree of supercooling, the sizes and shapes of the ice crystals and the degree of turbulence which governs the relative velocity between the ice crystals and the surrounding water.

From experiments in quiescent water supercooled to from slightly below  $0^{\circ}\text{C}$  to  $-3.0^{\circ}\text{C}$ , Arakawa (1954) found that the rate of growth of discoid crystals (more will be said on the shape of frazil crystals later in the text) varied in the range of  $0.1-5.0 \times 10^{-3}$  cm/s when nucleation took place on the surface. It was found that the rate of growth of the ice crystals indeed was a function of the degree of supercooling, the sizes and the forms of the ice crystals. The colder the water and the smaller the ice crystals, the faster was the growing rate. Under otherwise identical conditions, needle crystals and dendrite crystals (also see later in the text) grew faster than discoid crystals.

Based on experiments on discoid frazil crystals, Mason (1958) gave the following rates of growth of diameter of the crystals:

At 0.05°C supercooling,	0.5-1.3 x 10 <sup>-3</sup> cm/s
At 0.10°C supercooling,	1.0-2.5 x 10 <sup>-3</sup> cm/s.

Fernandez and Barduhn (1967) performed experiments by passing supercooled water over a stationary plate ice crystal with scalloped edges and observing its growth. They proposed the following empirical equation for the growing velocity of the crystal:

$$v_{\text{ice growth}} = A_i v^{1/2} (\Delta T)^{3/2} \quad (31)$$

where  $A_i$  is a constant which presumably depends on the form and the size of the crystal,  $v$  is the relative velocity between the ice crystal and the flow and  $\Delta T$  is the degree of supercooling. Although the above equation was derived for stationary ice crystals, it may be used for frazil crystal growth if  $v$  is considered as the relative velocity between the ice crystal and the ambient fluid due to turbulence. A qualitative conclusion which becomes immediately clear from the above equation is that for anchor ice, because its relative velocity with respect to the ambient flow is much greater than that of the frazil crystals, a much faster growth rate should be expected. This conclusion, in fact, is confirmed by field observations.

Coming to the third factor on the multiplication of frazil crystals, it was learned from the theory of frazil nucleation earlier in the text that it depends on how fast secondary ice nuclei are produced by the breaking up of the existing frazil crystals (including the shedding of seed ice by the parent ice crystals) in the water. Since such a process accelerates with increased level of turbulence, the rate of multiplication of frazil crystals therefore also increases with the level of turbulence of the water.

Based on experiments, Carstens (1966) obtained the following empirical equation for the increase of frazil ice in water:

$$\frac{dM_i}{dt} \propto \frac{k}{H_L} M_i^{1/3} N^{2/3} Re^a \Delta T \quad (32)$$

where  $M_i$  is the mass of ice in the water,  $k$  is the thermal conductivity of the water,  $H_L$  is the latent heat of fusion of ice,  $N$  is the number of frazil crystals in

the water,  $Re$  is the flow Reynolds number,  $\Delta T$  is the degree of supercooling and  $a$  is a constant obtained experimentally for different flow conditions. The above equation may be rewritten as

$$\frac{dM_i}{dt} \propto \frac{k}{H_L} \left( \frac{M_i}{N} \right)^{1/3} N Re^a \Delta T \quad (33)$$

It is seen from the above equation that the rate of increase of frazil in the water increases with the number of the ice crystals  $N$ , the degree of supercooling  $\Delta T$ , the level of turbulence which is measured by the Reynolds number  $Re$ , and the size of the ice crystals which is given by  $M_i/N$  to the  $1/3$  power.

The rate of increase of frazil mass with the size of the frazil crystals is not necessarily in conflict with Arakawa's (1954) finding noted earlier that small frazil crystals grow faster than large frazil crystals. Although a larger crystal has a smaller growth rate in its linear dimension, because of its larger surface area, the rate of volumetric growth and, consequently, the rate of growth in mass, can be greater.

It should be pointed out that the above discussion and Eq. 33 are only true when the number of frazil crystals in the water is small so the diffusion of heat from a frazil crystal is not affected by the presence of other crystals. As the number of frazil crystals increases, at a certain point, the effective diffusion of heat from a crystal will be hindered by the presence of the others. Eventually, a saturation point will be reached at which further creation of secondary ice nuclei will have little effect on the rate of increase of frazil in the water. In other words, in a control volume, some time after the initiation of formation of frazil, the rate of latent heat liberated by the frazil crystals will reach a constant value determined by the degree of supercooling and the level of turbulence of the flow.

The conservation of heat when frazil is involved has been shown to be governed by Eq. 2

$$\begin{aligned} \int_V \rho H_L \frac{\partial c_i}{\partial t} dV - \int_V c_p \frac{\partial T}{\partial t} dV - \oint_A \vec{q} \cdot \hat{n} dA \\ + \oint_A \rho H_L (c_i \vec{v}) \cdot \hat{n} dA - \oint_A c_p (T \vec{v}) \cdot \hat{n} dA = 0 \end{aligned} \quad (2)$$

in which the first term is the rate of heat liberation in the control volume because of frazil formation, the second term is the rate of heat absorption for increasing the temperature of the water in the volume, the third term is the net heat flux into the volume across the surface, the fourth term is the rate of heat left in the volume because of the outflux of frazil from the volume and the fifth term is the heat flux into the volume associated with the influx of water across the surface boundary. In the case of a pond or a long reach of a river, the fourth and fifth terms will be either zero or negligible in comparison with the other terms and thus may be dropped from the equation. As for the first term, according to the discussion in the last paragraph, it will approach a constant value some time after the onset of frazil nucleation and this constant value is determined by the degree of supercooling and the level of turbulence. The balance of the equation, therefore, is primarily achieved by the readjustment of the second term of the equation following changes in the third term. Following is the sequence of readjustment in the control volume following a perturbation:

For a control volume of frazil producing water at equilibrium, if the meteorological conditions are now changed so that the heat flux to the water is reduced, the third term of the above equation will be reduced. To compensate for this reduction, the second term of the equation will be increased or the rate of cooling of the water  $\partial T/\partial t$  will be more negative. This greater rate of temperature reduction means a higher rate of supercooling which, in turn, permits a higher rate of heat removal from the growing frazil crystals or a greater rate of frazil production  $\partial C_i/\partial t$ . A higher value of  $\partial C_i/\partial t$  means the first term of the equation is also increased which further helps to balance the equation or helps the control volume to reestablish equilibrium.

The above sequence of events occurs when the heat flux to the control volume is reduced. A similar sequence of events, but in the reverse order, will take place if the change in the meteorological conditions leads to an increase in heat flux to the water instead of a reduction.

Thus, it is seen from above that it is possible for the degree of supercooling of a frazil-producing water body to vary over a considerable range, contrary to the common belief that the water temperature will quickly return to the equilibrium temperature or very close to it following the formation of frazil ice in the water. For the Niagara River, it has been observed that the temperature of the water continued to lower to as much as  $-0.07^{\circ}\text{C}$  while frazil was being produced in the water (Ontario Hydro, 1967-70).



Before concluding this section, it should be mentioned that while all researchers agree that the turbulence level does affect the rate of growth of the frazil crystals, there are two schools of thought on whether the nucleation temperature is affected by the turbulence. Some (Osterkamp, 1978) consider that the turbulence level does not affect the nucleation of frazil and some (Michel, 1980) believe that there is important dependence of the threshold nucleation temperature on the level of turbulence.

#### 4.0 METAMORPHOSIS, GROWTH AND EVOLUTION OF FRAZIL

##### 4.1 Basic Shapes of Frazil Crystals

Frazil either appears as small spicules or as small discoids in nature. Fig. 4a is a picture showing the spicule or needle frazil crystals. The light object in the picture is about 2 cm long. Fig. 4b (Ontario Hydro, 1969; Arden and Wigle, 1972) is a picture showing the discoid ice crystals. The mesh size in the picture is about  $1\text{ mm}^2$ . The thickness of discoid frazil crystals usually varies between 0.05 to 0.5 mm. Besides being different in shape, needle frazil is also different from discoid frazil in that it does not stick to underwater objects as discoid frazil does at its early stage of formation.

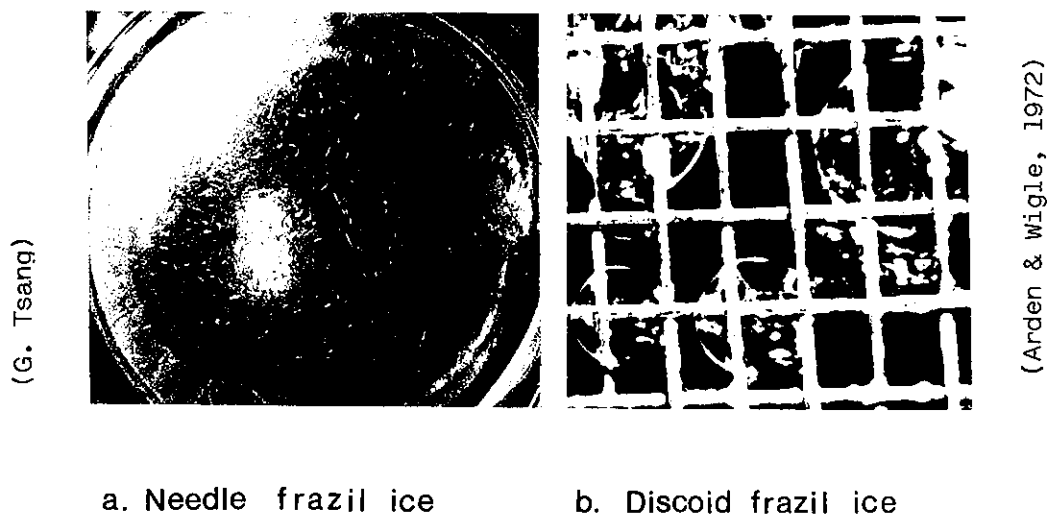


Fig. 4 Frazil ice crystals found in nature

Experiments by Arakawa (1954, 1967) in quiescent water showed that when the degree of supercooling is small and the nuclei available are abundant, frazil tends to assume the discoid form. However, when the water is more than  $0.9^{\circ}\text{C}$  supercooled, only needle frazil will be formed. One may view the formation of needle frazil as nature's way of enhancing heat dissipation from the growing frazil crystals. At the early stage of frazil formation not long after nucleation, according to the nucleation theory presented earlier, the frazil

crystals are necessarily circular in shape (i.e., as discoids) so as to have the least surface area and consequently the least surface energy. When the number of nuclei is large and the ambient water is relatively warm, the rate of heat dissipation by each crystal is low and the crystals can continue their growth as discoids. However, when the number of nuclei is small and the degree of supercooling is high, the rate of heat dissipation by each crystal will be high. To better diffuse this high rate of latent heat liberated, the crystals effectively increase their surface area by assuming the spicule form. The above also explains why in nature needle frazil crystals are generally smaller than discoid frazil crystals because only with a small volume will the surface area/volume ratio be large enough for effective heat dissipation from the frazil crystals.

In Arakawa's 1954 experiments, semicircular crystals were also noted. Such frazil crystals, however, were never observed in nature in noticeable quantity.

In nature, when frazil is being produced, the temperature of the water is seldom less than  $-0.1^{\circ}\text{C}$  and the frequency of occurrence of discoid frazil is much higher than that of needle frazil. There have been cases, however, where needle frazil was produced in a river at a temperature only slightly below  $0^{\circ}\text{C}$  while discoid frazil was being produced elsewhere in the same river at greater supercooling (Ontario Hydro, 1969). Apparently, more research is needed to understand the conditions under which discoid frazil and needle frazil will form.

Thermodynamics also governs the final growth of discoid frazil crystals. Because the circular shape possesses the least surface energy, under normal circumstances, a discoid frazil crystal will remain a discoid. Under favourable conditions, a discoid crystal can grow to about 8 mm in diameter and still retain its discoid shape. However, as the crystal continues to grow to a certain point, the surface area/volume ratio of the crystal will be sufficiently low that a circular boundary can no longer adequately diffuse the latent heat released by the growing crystal. To overcome this difficulty, local irregularities begin to form to give a larger surface area for better heat dissipation. Figure 5 (Ontario Hydro, 1970) is a photograph showing the growth of a frazil crystal from the circular form to the irregular form. The crystal shown is several mm in diameter. The circular core of the crystal showing the original shape of the crystal is clearly visible in the picture, indicating that in addition to local

growths at the boundary, the crystal also thins down at the edges, all for the benefit of giving a larger surface area/volume ratio.



(Ontario Hydro, 1970)

Fig. 5 Growth of frazil ice crystal from circular form to irregular form

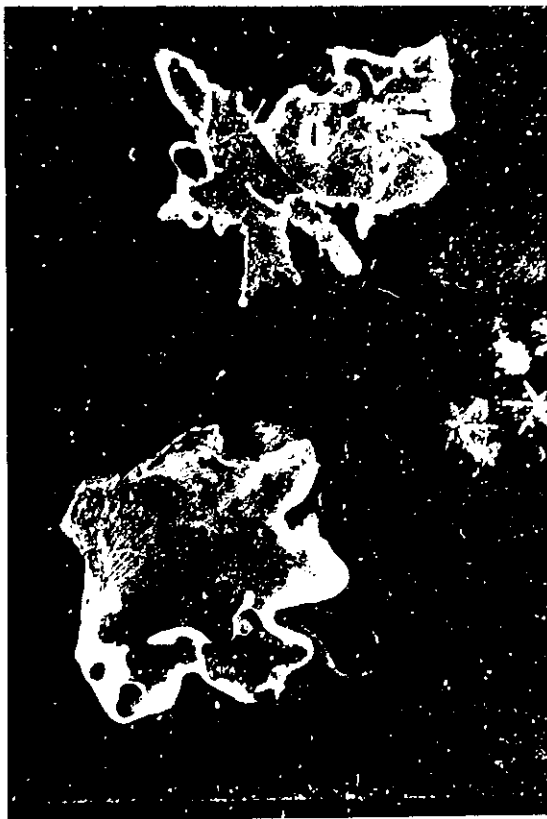
From the above discussion, one sees that both the formation of needle frazil crystals and the growth of discoid crystals from the original circular shape to an angular shape are for better dissipation of the latent heat. The angular crystals eventually grow to the dendrite form which can be considered as spicule growth in different directions.

#### 4.2 Formation and the Basic Forms of Flake Ice

It was mentioned earlier that intense long wave radiation plus evaporative and convective heat losses from the water surface can produce a thin, supercooled surface layer overriding a water body whose temperature is still above freezing. In this thin, supercooled layer, ice may nucleate. If the water is quiescent, a thin static surface ice sheet will form. However, if the water is turbulent, ice platelets or flakes will be produced. Flake ice, thus may be considered as an ice form between the static surface ice and the frazil that formed uniformly in the water. As mentioned earlier, however, Kivisild (1970) included flake ice in the domain of frazil.

Flake ice generally assumes three basic forms as shown in Fig. 6. In Fig. 6a (Ontario Hydro, 1970), the first, leaf-like basic form is shown. The crystals in the picture were about 1.25 cm across. In Fig. 6b (Ontario Hydro, 1970; Arden and Wigle, 1972), in the top left corner, the second, rectangular basic form is shown. One sees that one side of the crystal has saw-toothed edges, indicating that this is the side of crystal growth; the saw-teeth make the diffusion of the latent heat liberated by the crystal easier. The shown crystal was about 2 cm long. The crystal in the middle of Fig. 6b shows the third basic form, the needle form. The back of the needle usually thickens to a thickness about 2 to 3 times the thickness of the main plate, in the form of a rib. It is seen from the picture that one side of the needle crystal is also saw-toothed, indicating the places of fast ice growth. In the bottom right corner, one sees that several flake ice crystals of different basic forms were frozen together.

(Ontario Hydro, 1970)



a



b

(Arden & Wigle, 1972)

Fig. 6 Flake ice and its basic shapes

This is how flake ice forms and behaves. As a turbulent water body is gradually cooled down, the surface layer will first reach the nucleation temperature because it is in contact with the cold air and because the long wave radiation heat loss is confined to it. Ice, therefore, first nucleates on the surface. While the turbulence prevents the growth of the surface ice into large sheets, the stable stratification produced by cooling water from the top near the freezing point gives time for the ice crystals to grow into flakes. Because this surface supercooled layer is thin, the ice flakes are necessarily thin. While ice flakes are produced on the surface, no frazil ice is produced in the lower layers. The ice flakes can be entrained by the turbulent flow to the lower layers, where they may begin to melt because of the warmer surrounding water. However, they will resume their growth after refloating to the surface.

The thin, supercooled surface layer does not always contain the same water parcels. As a consequence of turbulence, the warm water from below continuously replaces the cooled water in the surface layer. This mass transport process, in fact, accounts for the ultimate cooling of the whole layer to the freezing or supercooled temperature. Thus, as continuing cooling takes place, gradually the surface supercooled layer will be thickened and the condition for flake ice formation no longer remains. The ice formed in the thick, supercooled layer, then, will be the conventional frazil.

According to the above discussion, one sees that the concentration of flake ice suspended in the flow should reach the maximum value just before the production of frazil. This, in fact, was verified to be the case by field observations in the Niagara River (Ontario Hydro, 1970). From the above, one can also see that depending on time and the hydrometeorological conditions, flake ice concentration in a flow can be substantial and can outweigh the presence of frazil.

It may be added that in supercooled water, flake ice can continue to grow. The flakes also become active by sticking to underwater objects or to each other. In other words, flake ice behaves as frazil in supercooled water.

#### 4.3 Evolution of Frazil from Crystals to Floes

After their formation, frazil crystals begin to agglomerate, first into clusters, then into flocs, and float to the surface. In still water, the rising velocity of discoid frazil crystals of 1 mm diameter has been found to be about

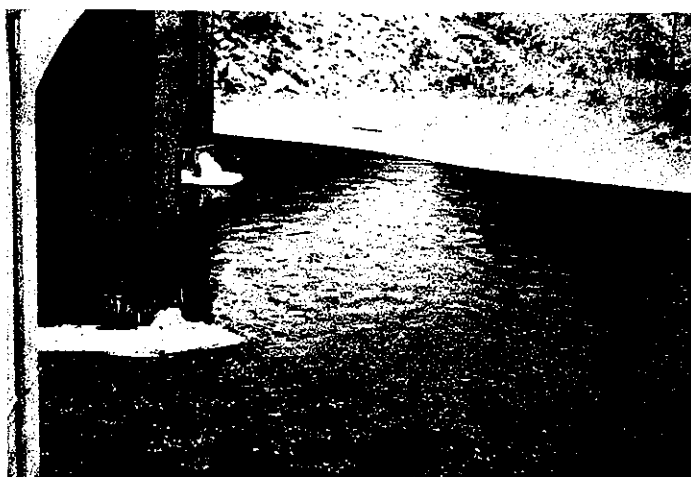
0.2 cm/s (Arakawa, 1954). For clusters and flocs, no measurement has been made. At the same time, the turbulence of the flow, breaks up the agglomerations and brings the flocs and clusters back into the flow. While the fusing together and the interlocking of the frazil crystals point to the direction of larger flocs, the spatial variation of the flow velocity causes the large flocs to be torn up into small clusters. It is a common sight in rivers at local constrictions to see large and thick frazil flocs being stretched and broken up into small clusters or to disappear in the turbulent flow altogether.

When frazil clusters and flocs are first formed, they are quite porous and have a density very close to that of the surrounding water, and so their movement is largely controlled by the turbulence of the flow. However, during the intervals when the flocs and clusters are on the surface and exposed to the cold air, the interstices inside the flocs (and clusters) are gradually frozen up and this gradually increases the buoyancy of the flocs. Gradually, the flocs become more and more buoyant and respond less and less to the turbulence of the flow. At a certain stage, the frazil agglomerations will stay mainly on the water surface and are known as frazil slush.

The time involved for frazil to evolve from crystals to slush depends on the turbulence state of the flow and the meteorological conditions above the water. The turbulence level also affects the compactness of the frazil flocs. The more turbulent the flow, the more compact are the frazil flocs. The frazil flocs also assume a more spherical shape in a more turbulent flow.

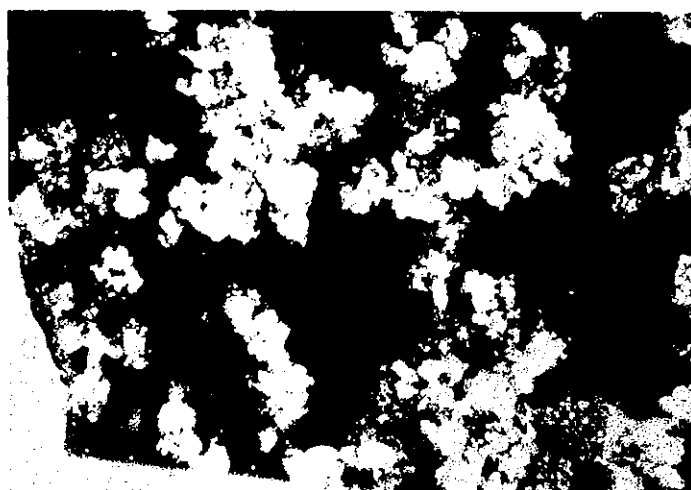
Figure 7 consists of photographs of frazil flocs in nature. The flocs are at their late stage of evolution. While Photograph a shows the flocs as seen from the bank, Photograph b gives a close-up look of the flocs and Photograph c is a blowup of a small floc. The scale in Photograph c is in millimetres. It is seen from this photograph that the frazil crystals are discoids. The discoids stick together chiefly by fusing and are aided by interlocking. From the circular shape of the crystals, one sees that the frazil crystals agglomerate at an early stage, before the crystals reach the irregular form.

Figure 8 is a photograph showing frazil flocs formed by needle frazil crystals. Comparing Fig. 8 with Fig. 7, one sees that needle frazil flocs are not as dense as discoid frazil flocs. Needle frazil flocs also show more density variations within a floc. A close look at the flocs would show that the agglomerations are formed by the interlocking of the needle ice crystals, and not by fusing together as in the case of discoid frazil flocs.



(Tsang & Beltaos)

a. Frazil ice floes in river



(Tsang & Beltaos)

b. Close-up look of frazil floes



(T. E. Wigle)

c. Blow-up of a frazil floe

Fig. 7 Agglomeration of discoid frazil ice





(G. Tsang)

Fig. 8 Needle frazil ice flocs in a flume (ignore large ice crystals formed on the glass wall)

In studying the formation of frazil, Michel (1967) found that frazil crystals (discoids) are very active at their early stage of formation in that they stick easily to each other and to underwater objects. A later study (Ontario Hydro, 1967-70) showed that frazil (discoids) remains active as long as the water is supercooled. It was mentioned earlier that during the formation of discoid frazil crystals, the diffusion of heat from the ice crystals is not rapid. The heating up of water therefore is slow and this leaves time for the water to remain supercooled and the crystals to have the chance to stick to each other. The above explains why fusing is the main mechanism of bonding for discoid frazil flocs. The discoid geometric shape of the ice crystals is also more conducive to the formation of more compact agglomerations. For needle frazil crystals, it was mentioned earlier that the diffusion of heat from them is rapid. The water, at least the part immediately surrounding the crystals, therefore is warmed up rapidly. The supercooled time of the ice crystals therefore is short and this does not give much time to the needle crystals to stick together. From the above, one sees that needle frazil crystals do not fuse to each other because of the lack of supercooling time, rather than the shape of the ice crystals per se. Because the needle geometric shape is conducive to interlocking, interlocking becomes the main mechanism in forming needle frazil flocs.

It should be mentioned that the frazil crystal concentration in water is high. In suspended form, a crystal concentration of  $10^6/\text{m}^3$  has been reported by Gilfilian et al (1972). However, the weight concentration of frazil in water is low. In suspended form, Ontario Hydro measurements (1970) showed that 0.5 percent appears to be the upper limit. The low weight concentration of frazil is also true for frazil flocs. A seemingly very thick frazil floc may turn out to contain only one or two percent frazil by weight. Although the weight concentration of frazil in a floc is low, the spongy structure of the floc is very effective in inhibiting water movement in the interstices of the floc and this permits the formation of static ice in the interstices on the surface.

It was mentioned earlier that frazil slush is formed when frazil flocs float to the surface. If the slush ice stays on the surface long enough, a continuous ice sheet will be formed on the top, overriding a porous mass of frazil flocs. The ice sheets so formed are known as frazil pans. At places where the variation of velocity with depth is large, the overridden frazil flocs may be torn away from the sheet ice on the top, to reemerge elsewhere and become new nursing grounds of frazil pans. Often, as the frazil pans move about in the water

and grind among themselves, they will attain a circular form with upturned edges and are known as pancake ice. Figure 9 is a photograph showing pancake ice formed in a river. The size of the frazil pans and the subsequent pancake ice is a function of the original size of the frazil floc agglomerations, the quantity of frazil that is in the water and may later add to the ice pan, and the hydro-meteorological conditions.

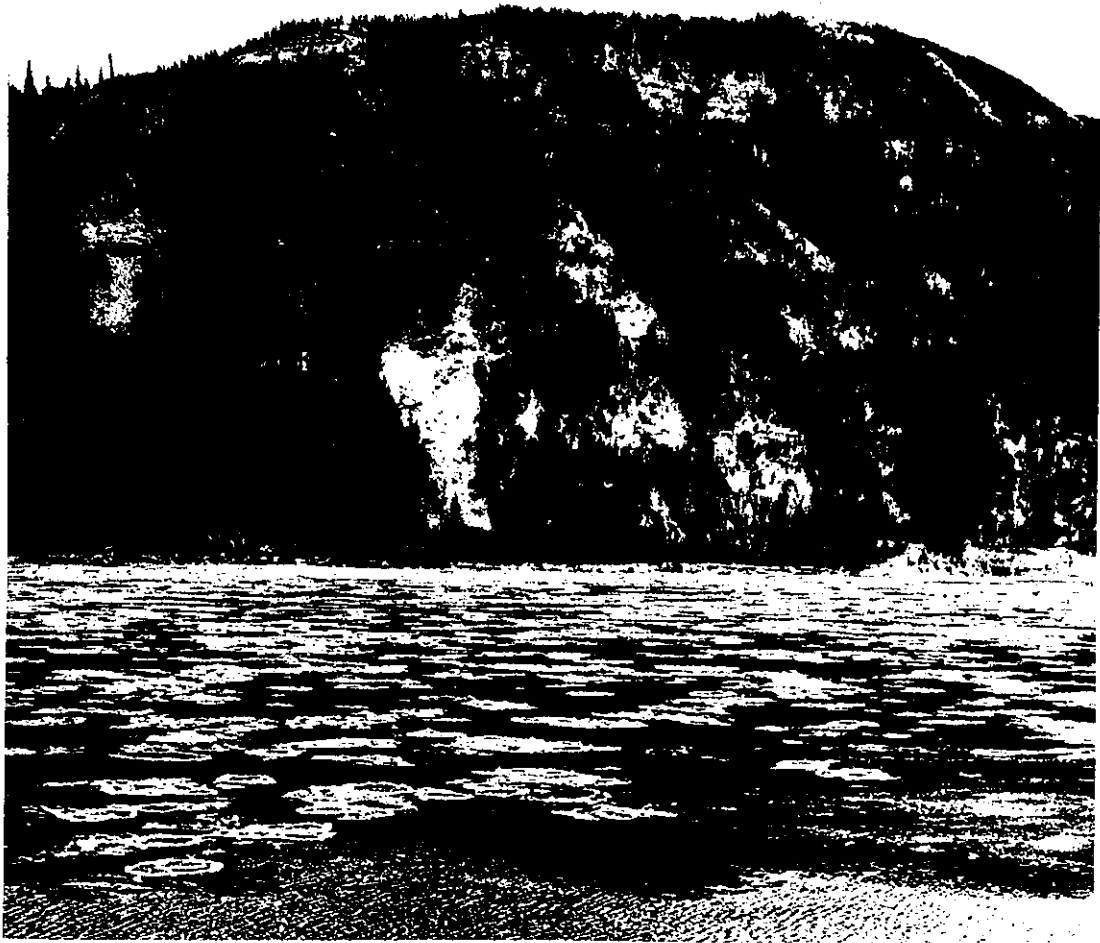
According to the above description of how frazil pans originate, one can see that the initial thickness of frazil pans is not great, usually measured in fractions of a centimetre only, although the parent frazil flocs underneath can be tens of centimetres thick. The pans thicken by freezing water and frazil to the underside of them.

The freezing together of frazil pans (including pancake ice), produces frazil floes. Frazil floes are formed in reaches where the flow is slow and the contacting frazil pans have more time to freeze together.

It should be pointed out that the production of frazil, the formation of frazil clusters and flocs, the production of frazil pans and pancake ice, and the fusing together of frazil pans to form frazil floes are not set at distinct stages, but overlap and often happen together. Frazil flocs, in addition to forming frazil pans, also cling to border ice and contribute to the growth of the border ice. Because of the diurnal cycle of frazil production, border ice on natural rivers is often seen to be composed of strips of different shadings, representing frazil additions of different days. As to frazil pans and frazil floes, they are the main building blocks for forming an ice cover over a river, especially a wide one, as will be shown later.

Although the above descriptions are for frazil ice in rivers, the same evolution processes are involved for frazil ice in lakes, only that there the turbulence is produced by wind rather than by the flow.

Also in the above discussion, frazil is assumed to form in fresh water. This condition is not necessary as frazil has been observed to form in the Antarctic under the ice cover (Robilliard, 1980; personal communication). In the Antarctic, the severe cold can supercool the seawater under the ice cover so an open water is not a necessary condition for supercooling the water which is a necessary condition for frazil formation. However, it was learned earlier that turbulence is the other necessary condition for frazil formation and, under the Antarctic ice cover, the turbulence level should not be high. The turbulence



(S. Beltaos)

Fig. 9 Pancake ice in a river

level required for frazil formation in seawater therefore is an area of further research.

#### 4.4 Evolution of Frazil in Niagara Rivers; A Field Example

The evolution of frazil and the time scale involved can be illustrated by the photographs shown in Fig. 10. The photographs were taken of the upper Niagara River (Ontario Hydro, 1967) from upstream to downstream near noon, always looking upstream. The upper Niagara River is about 30 km long. Its depth varies from about 4 metres to about 12 metres and its width averages about 750 m with the narrowest part of 550 m at the first bridge shown in the map in Fig. 10. The flow velocity of the river varies from a low of about 0.3 m/s at the ice boom to a high of about 3 m/s at the narrows at the first bridge. It may be pointed out that the narrows also has the shallowest depth. It takes about 8 hours for water to flow through the river. The reaches covered by the photograph are also indicated on the map. Because of the ice boom, the ice in the lake is prevented from entering the river. Field measurements of the water temperature at the ice boom showed that the water temperature is always above 0°C. Thus, at the entrance to the river, the river is ice free and above freezing.

It is seen from Fig 10a that, as the water flowed from the ice boom to the first bridge, it mainly underwent a cooling process so no surface ice is noticeable in the picture in the stretch from the boom to the first bridge. On-site observations, on the day the photographs were taken, showed that the water reached the nucleation temperature at a short distance from the first bridge as evidenced by the appearance of the first frazil.

At the first bridge and the stretch immediately following it, frazil was continuously produced. However, the fast current there prevented the frazil crystals from agglomerating into fair sized flocs that possess the necessary buoyancy to float to the surface, so the frazil remained in the suspended state and cannot be detected from the photograph.

Further downstream, as the flow slowed down, the frazil had a better chance to agglomerate and float to the surface. The presence of frazil clusters and flocs in the stretch immediately upstream from the second bridge can be detected from the lighter colour in the picture.

Downstream from the second bridge, the flow slowed down further and the presence of frazil flocs became more noticeable. Most frazil flocs were

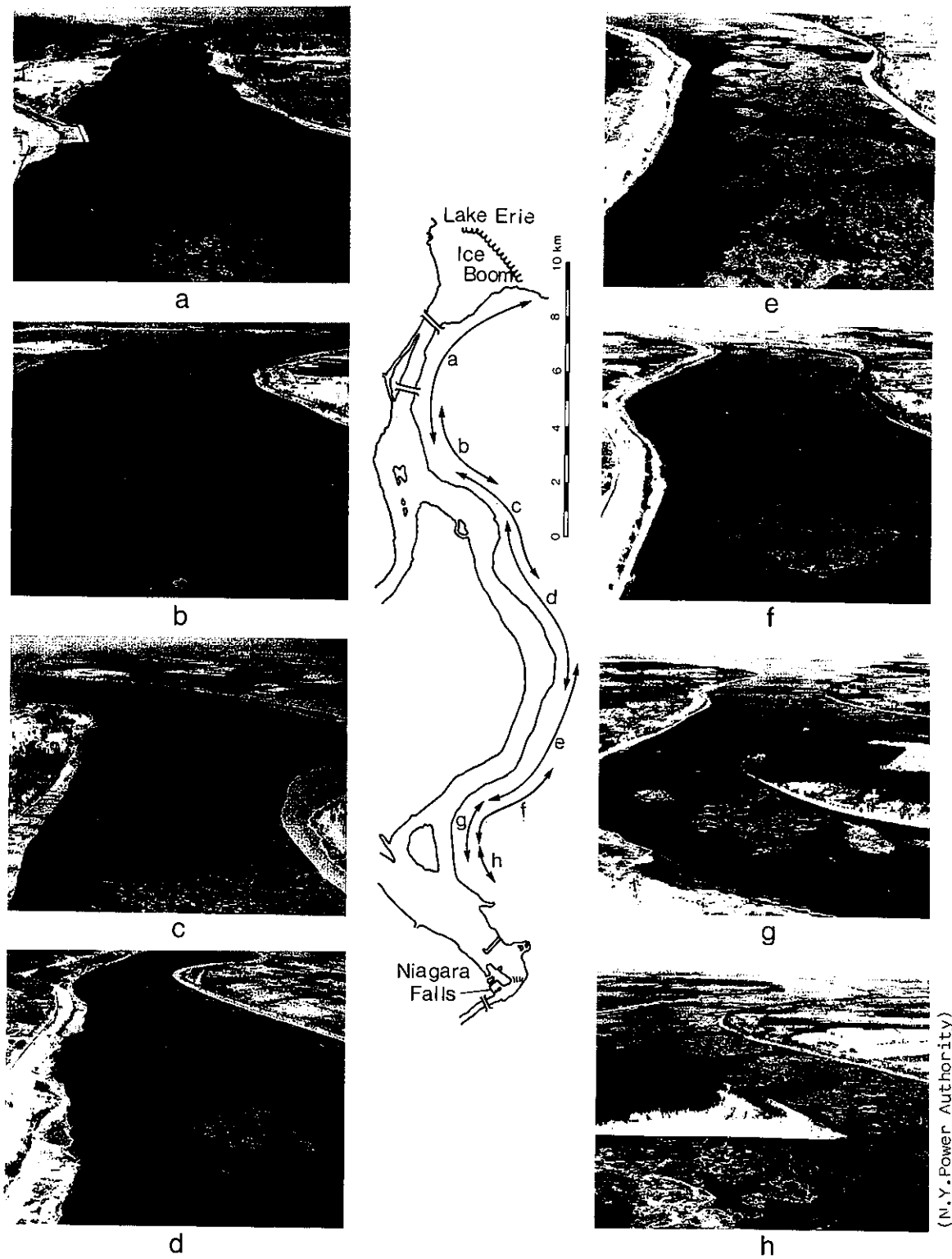


Fig. 10 Evolution of frazil ice in river (Niagara River)

fully immersed in the water. However, some of the flocs have agglomerated to a sufficiently large size so part of them extended into the air as is seen from the lower part of the picture near the centre. At this point, the formation of frazil pans from frazil flocs also began to take place.

In Fig 10b, more frazil pans are seen on the surface. The presence of frazil flocs, now grown into slush agglomerations, can also be delineated by their lighter colours. Because of the small number of frazil pans and the short time after their birth, there was insufficient chance for them to collide and grind among themselves, so the frazil pans were of irregular form, instead of the circular form.

In Fig. 10c, one sees now that the ice pans covered large parts of the water surface. At the bottleneck reach (see the map), the surface concentration was even higher. The increased collision and grinding of the frazil pans have caused them gradually to assume the generally circular form. In the picture, the formation of frazil floes by frazil pans sticking together can also be seen.

Coming out of the bottleneck, some well-defined frazil floes can now be seen from Fig. 10d. The shape of these newly formed frazil floes was generally irregular. Some water openings in the floes could be seen. The water movement in these openings was slow, favouring the formation of static ice.

Further downstream, the frazil floes grew to larger sizes by freezing to each other as may be seen from Fig. 10e. Many openings in the frazil floes were also frozen over. In the picture, the lighter shaded frazil slushes and the surface ice formed over them can also be seen, indicating that frazil was formed continuously all the way along the river.

In Fig. 10f, the ice floes are seen to have acquired the more matured, angular shape as a result of abrasion with the shore. The edges of the floes were now much better defined. Experienced observers can also tell that static ice, or black ice, has now been formed in all previous open water openings. The proportion of frazil flocs and slushes, has also been significantly reduced.

In Fig. 10g and Fig. 10h, no further maturing of the ice floes is noted. The presence of frazil flocs and slushes, however, can be seen to have increased, possibly due to the larger surface area of the river, and consequently more frazil ice production.

Although the frazil floes shown in Fig. 10 were quite large, they were, however, not thick. The thickness of the ice floes at the downstream end

of the river measured only about 5 cm. This ice thickness was produced at an air temperature of about  $-15^{\circ}\text{C}$  and with a net long wave radiation heat loss rate of about  $-10 \text{ cal/cm}^2/\text{hr}$  at night. On the day the photographs were taken, the sky was overcast but no wind data were taken.

It was mentioned earlier that frazil pans and floes are ultimately evolved from frazil ice crystals. Field studies conducted in the Niagara River (Ontario Hydro, 1969) showed that the frazil crystals not only floc together to form the sponge like agglomeration which permits the formation of static ice in the interstices, but actually take part in forming the surface ice crust themselves. It was found in the above study that for surface ice sheets less than 0.3 cm thick (1/8 in.), they were almost entirely composed of mature frazil discoids with dendrite edges. The discoids froze together in an overlapping fashion. For thicker ice sheets, however, examination of the cross sections showed that they were close to black ice, indicating the progressively more important role of freezing water to the underside of ice sheets in thickening the sheets. The relative importance of the roles played by conductive freezing and frazil accumulation in the thickening process of frazil floes can be studied by placing the cross-sectional specimens of frazil floes under a polarized light.

Fig. 10 shows the typical situation of frazil production and evolution for an outlet river of an ice-covered lake and, to a certain degree, for the open-water section of a river downstream from an ice-covered section. Under the ice cover, because of the geothermal heat input and the reduced heat loss to the atmosphere due to the insulation of the ice cover, the water remained above freezing. As this warm water emerges into the open section it will be cooled gradually and the formation and evolution of frazil will take place subsequently.



## 5.0 ACCUMULATION, TRANSPORT AND DEPOSITION OF FRAZIL IN RIVERS

### 5.1 Accumulation of Frazil in the Form of River Ice Cover

It was mentioned in the last chapter that frazil flocs contribute to the growth of border ice and frazil pans and floes are building blocks of ice covers, especially on wide rivers. To initiate an ice cover on a wide river, a barrier across the river or an ice bridge is needed. An ice bridge may be formed at a control section where the river is narrow and deep and the flow is slow. After cold spells when the surface concentration of ice on the river is high, the surface concentration at the control section may reach 100 percent. If the weather remains cold, there is the probability for the surface ice jamming in the control section to freeze together and form an ice bridge. It is easy to see that ice bridges of this kind are likely formed by frazil slush, pans and floes. Of course, the static ice cover formed over a quiescent reach of a river may also serve as an ice bridge.

When frazil slush, pans and floes drift to an ice bridge, or the leading edge of an ice cover, they may either be stopped by the barrier or may be swept under it. If the ice and hydrodynamic conditions are such that the oncoming ice is stopped by the barrier, the ice will accumulate in front of the barrier and gradually progress upstream. This way of ice cover growth is known as ice cover formation by juxtaposition and is a very important way of ice cover formation on wide rivers. It is also a very fast process. Cousineau (1959) reported a field case in which 40 km of ice cover was formed in one day in such a way.

Whether the drift frazil slush, pans and floes will be stopped by an ice cover or not can be determined by studying the stability of the leading edge of the ice cover. By writing the Bernoulli equation between a point upstream of the leading edge of the ice cover and a point below it and using the assumption that the leading edge will be unstable if it becomes submerged underwater, the following criterion for the stability of the leading edge can be derived (Michel, 1978):

$$\frac{V}{\sqrt{gY}} \leq \sqrt{2(1 - \rho'/\rho)(1 - e)(h/y)} [1 - (h + \xi h)/y] \quad (34)$$

where  $V$  and  $Y$  are the flow velocity and the flow depth upstream of the leading edge respectively,  $\rho$  and  $\rho'$  are the density of water and solid ice respectively,  $h$

is the thickness of the leading edge,  $e$  is the porosity of the leading edge, expressed as the ratio of volume of water to the volume of water and ice,  $g$  is the gravitational acceleration,  $\xi h$  is the thickness of the separation boundary layer under the leading edge and  $y$  is the depth of flow under the leading edge not counting  $\xi h$ . It may be noted that an equation of essentially the same form as Eq. 34 was also derived by Kivisild (1959).

The left hand side of Eq. 34 can be recognized to be the Froude number of the upstream flow. Equation 34 thus states that if the upstream Froude number is equal or less than the value given by the right hand side of Eq. 34, the leading edge of the ice cover will be stable. Because the right hand side of Eq. 34 decreases with the increase of porosity  $e$ , one can see that the more porous the frazil slush, pans and floes, which, when momentarily contained by the ice cover, will become the leading edge of the ice cover, the easier will they be swept under the ice cover by the current. Thus, under a certain set of flow conditions, one may see that, while frazil floes and pans (which are denser) are stopped by the leading edge of the ice cover, frazil slush (which is more porous) is swept by the current under the ice cover. Likewise, for the same leading edge subject to the same hydrodynamic conditions, it may be able to stop the drift frazil flocs when the weather is cold and the flocs are thick, and loses its containing capability when the weather is mild and the frazil flocs formed upstream are highly porous. Similar situations may also occur with frazil pans and frazil floes.

For a deep river, both  $h$  and  $\xi h$  are small compared to  $y$ , and  $Y$  and  $y$  are approximately equal. Eq. 34, thus is reduced to

$$V \leq \sqrt{2g (1 - \rho'/\rho) (1 - e) h} \quad (35)$$

The above equation shows that, for a deep river, the critical flow velocity is proportional to the square root of the leading edge thickness  $h$ . Thus, for an unstable leading edge subject to a given velocity, as the oncoming ice is swept under it and, as a consequence, increases its thickness, the critical flow velocity will also be increased. In other words, an initially unstable leading edge can reestablish its stability by thickening itself and by so doing permit further growth of the ice cover by juxtaposition. From the above, one sees that the thickness of the ice cover of a deep river formed by frazil accumulation will not be uniform,

but will vary from point to point. At sections where the flow velocity is high, the ice cover will be thick and at sections where the velocity is low, the ice cover will be thin.

Equation 35 may also be used for ice cover formation over lakes or seas. In such a case,  $V$  may be approximately considered as the surface current.

The re-establishment process discussed above, however, does not go into an endless circle. The plotting of the critical Froude number  $Fr = V/\sqrt{gY}$  against  $h/y$  according to Eq. 34 would show that there exists a maximum critical Froude number. By equating  $dFr/d(h/y)$  to zero and using a value of 0.916 for  $\rho'/\rho$ , this maximum critical Froude number can be shown to be:

$$Fr_{\max} = 0.112 \sqrt{1 - e} / \sqrt{1 + \xi} \quad (36)$$

When the Froude number in a river is greater than the above value, all the oncoming ice would be swept under the ice cover regardless of the thickness of the leading edge. While the functional form of the above equation has been proven to be valid, field experience showed that the constant 0.112 should be modified to 0.158. Equations 34 to 36 (with the constant equal to 0.158) have been widely used by practising engineers, usually with appropriate factors of safety.

It may be pointed out that Eqs. 34 and 36 are for windless conditions only. Under windy conditions, the critical surface velocity and the maximum critical Froude number will be smaller.

It should also be noted that even when the flow Froude number is higher than the critical value, under exceptional conditions such as when the rate of drift ice supply is greater than the rate of ice being swept under the ice cover, the leading edge of the ice cover can still propagate upstream. After the added ice cover is solidified by the cold weather, reducing the supply rate may not lead to the collapse of the ice cover.

## 5.2 Transport and Deposition of Frazil under Ice Cover

The frazil slush, pans and floes swept by the current under the ice cover will be transported by the current along the underside of the ice cover. The frazil crystals and clusters that are suspended in the water and flow with the water under the ice cover will also add to the ice transported along the underside

of the ice cover as they agglomerate and float up to the ice cover. At places where the adhesive force between the transported ice and the ice cover is greater than the drag force on the ice by the flow, the transported ice will be deposited. The adhesive force is the sum of the friction force between the transported ice and the ice cover and the fusion bond as the moving ice tends to stick to the ice cover. Because the frazil ice moving under the ice cover undergoes continuous metamorphological changes, the adhesive force is a variable depending not only on the hydrodynamic conditions of the flow, but the meteorological conditions above the ice cover also. The drag force on the frazil ice also is varied because of the continuous density and form changes of the frazil agglomerations. Under given ice and meteorological conditions, however, there exists a critical velocity. If the flow velocity is less than this critical velocity, the transported ice will be deposited onto the underside of the ice cover.

Everything being equal, the transported ice will first be deposited at the leading edge of the ice cover because it is near the source of the transported ice supply. Once deposition has taken place, more ice will be added onto it because the surface of the new ice deposition usually is rougher than the original undersurface of the ice cover; it is also spongy so that the transported ice can cling to it more easily. The deposition of ice to the underside of the leading edge continues until the local flow velocity is increased to the critical velocity. Besides adding to the undersurface of the ice accumulation, the transported ice is also deposited to the wake of the accumulation where the velocity is low. This causes the gradual displacement of the wake or the growth of the frazil accumulation in the downstream direction.

The growth in thickness and the growth in length of an ice deposition go hand in hand. For an ice deposition, as its thickness is increased to the point that the velocity of the underflow has reached the critical value, ice no longer can be deposited on the bottom but to the wake of it only and this lengthens the length of the deposition. However, as the deposition lengthens, the resistance to the flow is also increased and this causes a reduction in the flow rate, which in turn reduces the flow velocity under the ice deposition and permits renewed deposition of ice onto the bottom of it to increase its thickness. The thickening and lengthening of the ice deposition therefore progress together and not as independent events.

Field measurements showed that frazil can be transported under the ice cover by the current for a long distance. However, once deposited, it will remain where it is and will not move like sediments on the river bed. The undulation sometimes shown on the underside of an ice cover is the result of thermal erosion of the ice cover by the warm water and is not the remains of frazil ice dunes. Field measurements by Tsang and Szucs (1972) showed that frazil accumulations under the ice cover can be completely eroded away by the flow but will not move as dunes. The reason that frazil accumulations do not move as sediment dunes do is because of the continuing morphological changes of the frazil ice so that the bond between neighbouring frazil crystals is much stronger than the bond between neighbouring sediment particles.

### 5.3 Hanging Dams

#### 5.3.1 Hanging dam and the factors controlling its growth and formation

A massive accumulation of ice under the ice cover is known as a hanging dam. According to earlier description on the deposition of frazil onto the underside of the ice cover, one sees that a hanging dam usually initiates from the leading edge of the ice cover and propagates in the downstream direction as reported by Michel (1967). The thickness of a hanging dam is controlled by the critical velocity which is a function of the state of the transported ice, the state of the hanging dam and the meteorological conditions above the ice cover. Based on hanging dam data obtained from La Grande River, Michel and Drouin (1974) showed that the critical velocity for narrow sections of the river was from 0.5 to 1.0 m/s with an average value of about 0.9 m/s. The critical velocity was time dependent, decreasing from a value of about 0.9 m/s at the beginning of the winter to a value of about 0.6 m/s at the end of the winter. For wide sections of the river, a smaller critical velocity was found, varying in the range of 0.5 to 0.8 m/s. This critical velocity also decreased with the progress of the season. It should be noted that the velocities quoted above are average velocities. Taking into account the areas in the cross section where the velocity is low or negligible because of back eddies etc., Michel and Drouin recommended a value of 0.9 m/s as the critical flow velocity for both wide and narrow sections of La Grande River if the hanging dams are mainly formed of frazil.

The formation of a hanging dam requires that:

- (1) There is an upstream source of abundant frazil supply; this means an open-water section where frazil flocs, pans and floes can be produced, and

(2) There is an ice cover for the frazil ice to be deposited onto.

Because, according to Eq. 36, only in sections where the flow Froude number is less than the maximum critical Froude number can an ice cover be formed and sections where the Froude number is greater than the maximum critical Froude number will always remain open; one sees that if a river is composed of sections with Froude numbers alternatively greater and less than the maximum critical value, the river will have alternatively open and ice-covered sections and such a river is most prone to the formation of hanging dams and floods caused by the damming of the flow by the hanging dams.

It should be noted that, as a consequence of the damming of the flow by the hanging dams and the backwater effect, the Froude number at the originally open sections may be reduced to subcritical values and ice covers may be formed over these sections. Thus, as the winter advances, the open area for producing frazil in the river is gradually reduced and the hanging dams in the river will grow no more or may even begin to be eroded away.

#### 5.3.2 Example of hanging dams formed in a river

La Grande River in northern Quebec is a river of alternative supercritical and subcritical Froude numbers (as defined by Eq. 36 and not in the usual open channel flow sense) and hence prone to the formation of hanging dams. Figure 11 is a diagram showing two hanging dams formed in that river (Michel and Drouin, 1974). It is seen from Fig. 11 that the main hanging dam was more than 16 km long and nearly extended to the bottom. The volume of frazil was calculated to be more than 56 million cubic metres, so the capability of the open water frazil producing stretch upstream of the hanging dam was enormous. It should be noted that point A shown in Fig. 11 was the point of the leading edge of the ice cover when the hanging dam was first initiated. As the hanging dam grew and the upstream stage rose because of the increased resistance, the upstream Froude number was reduced to less than the critical value and this permitted the progress of the leading edge to the point shown in Fig. 11.

Figure 12 shows the growth of the hanging dam at the cross section shown by the dash-dotted line in Fig. 11. It is seen from Fig. 12 that the frazil accumulation thickened as the winter progressed, supporting the earlier statement that a hanging dam grows in the downstream direction.

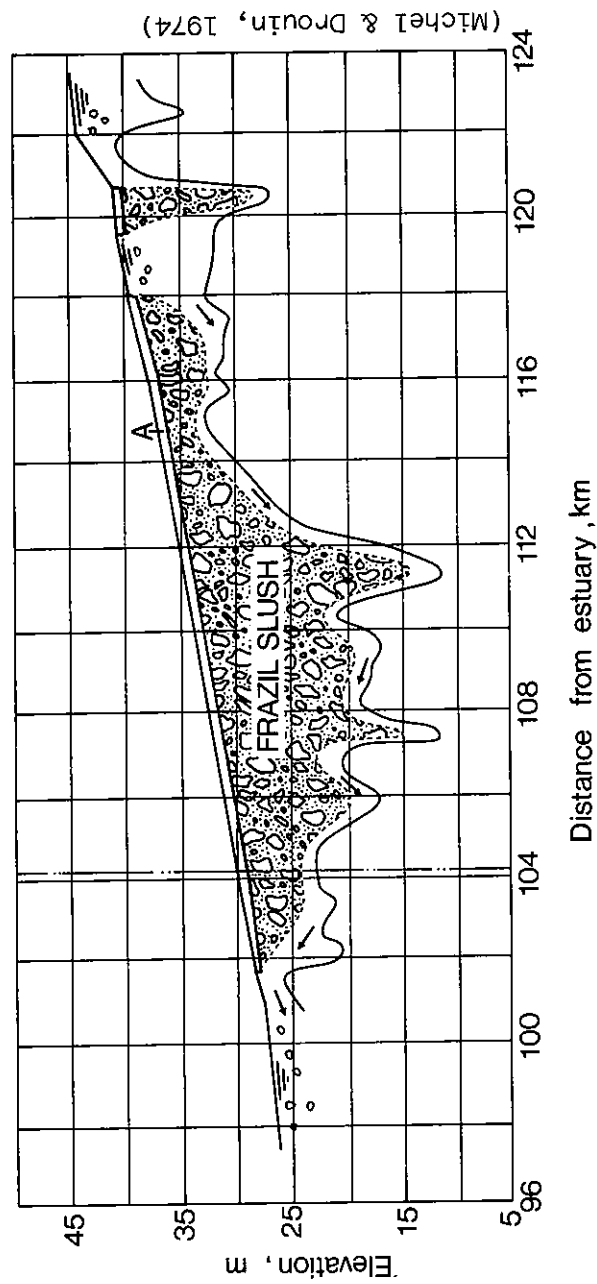


Fig. 11 Hanging dams in La Grande River, Feb. 1973

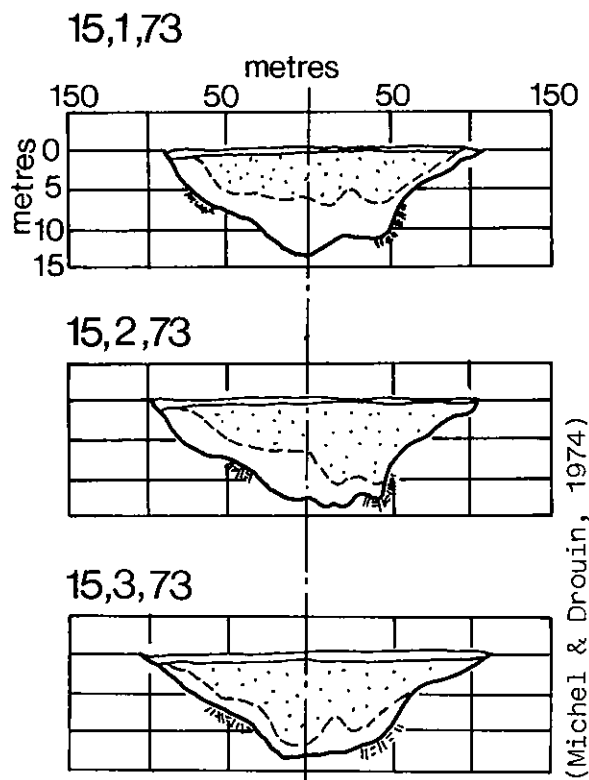


Fig. 12 Growth of frazil accumulation in hanging dam in La Grande River

The hanging dams shown in Fig. 11 were formed mostly of frazil. However, ice pans from border ice and other forms of ice were also found in the hanging dams, albeit in small quantities.

### 5.3.3 Formation of hanging dam in river mouth

Besides forming in the river itself, a hanging dam can also form in the river mouth when a frazil laden river discharges into a lake or a reservoir with an ice cover. For a fast flowing river that remains open during the winter, the amount of frazil ice produced can be huge and a large hanging dam can be formed. Such a hanging dam offers much resistance to the flow. In winter months, when the rate of discharge is small, the river mouth usually can handle the flow without having to substantially increase the upstream stage. In spring months, however, because of the high runoff of snow melt, the hanging dam can no longer pass the flow without causing upstream flooding. Because of the



relatively large size of such hanging dams, a high upstream stage often is required for their destruction and this means severe flooding.

Figure 13 shows a hanging dam that formed at the mouth of Moira River (Lathem, 1974) near the city of Belleville, Ontario. Although this river is quite small with a maximum width of only about 100 m and an average width much less than that, and a winter discharge of about  $25 \text{ m}^3/\text{s}$ , in contrast to a winter discharge of  $600 \text{ m}^3/\text{s}$  for La Grande River, the hanging dam was about 1 km long, extended from shore to shore of the river mouth with a width of nearly 300 m. Hanging dams have caused frequent flooding to the city of Belleville.

#### 5.3.4 Formation of hanging dam in local deepenings or enlargements

It was mentioned earlier that frazil ice is deposited by the flow at places where the flow velocity is less than the critical velocity. Because of this, for an ice-covered river, the places of local deepening or enlargement, where the flow velocity is reduced to less than the critical velocity, will be favourable spots for localized hanging dam formation. This indeed is the case as exemplified by the hanging dam shown in Fig. 14 which was formed in the Smoky River in Alberta in a sudden widening and deepening section (Beltaos and Dean, 1981).

#### 5.3.5 Morphological changes of frazil in a hanging dam

Frazil is not at a stable state but undergoes continuous morphological changes. This is true even after frazil has been deposited under the ice cover to form a hanging dam. In the hanging dam, the frazil crystals gradually change their form from discoids and spicules to the granular form with a mean diameter of about 1-2 mm. Thus, when a core is taken of a hanging dam, one would find that it is composed mainly of granular crystals, especially if the sample is taken towards the end of the season. The larger ice platelets, however, are morphologically stable and change little from their original forms in the hanging dam. A continuous record of the metamorphological composition of the ice crystals in a natural hanging dam, so far, does not exist in the published literature.

#### 5.3.6 Density and strength of hanging dam

Because of the metamorphological changes taking place in a frazil pack, the density, the shear strength and other physical properties of the frazil

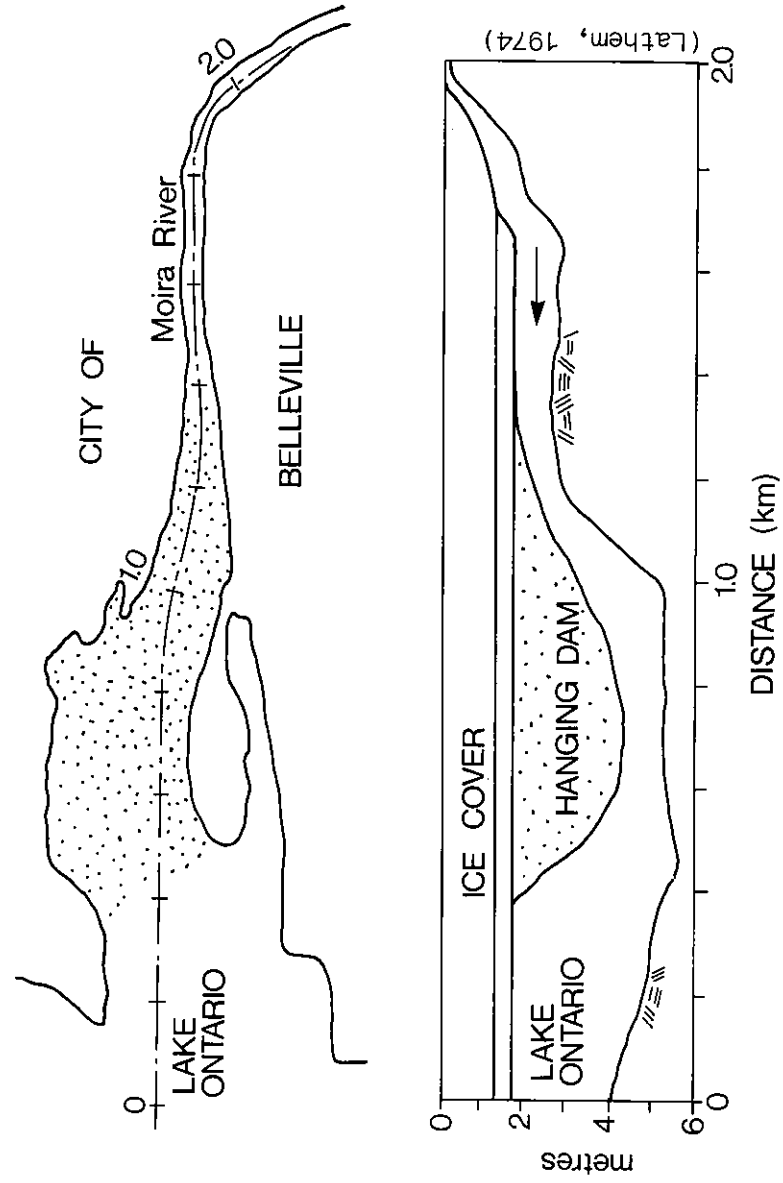


Fig. 13 Example of a hanging dam at a river mouth

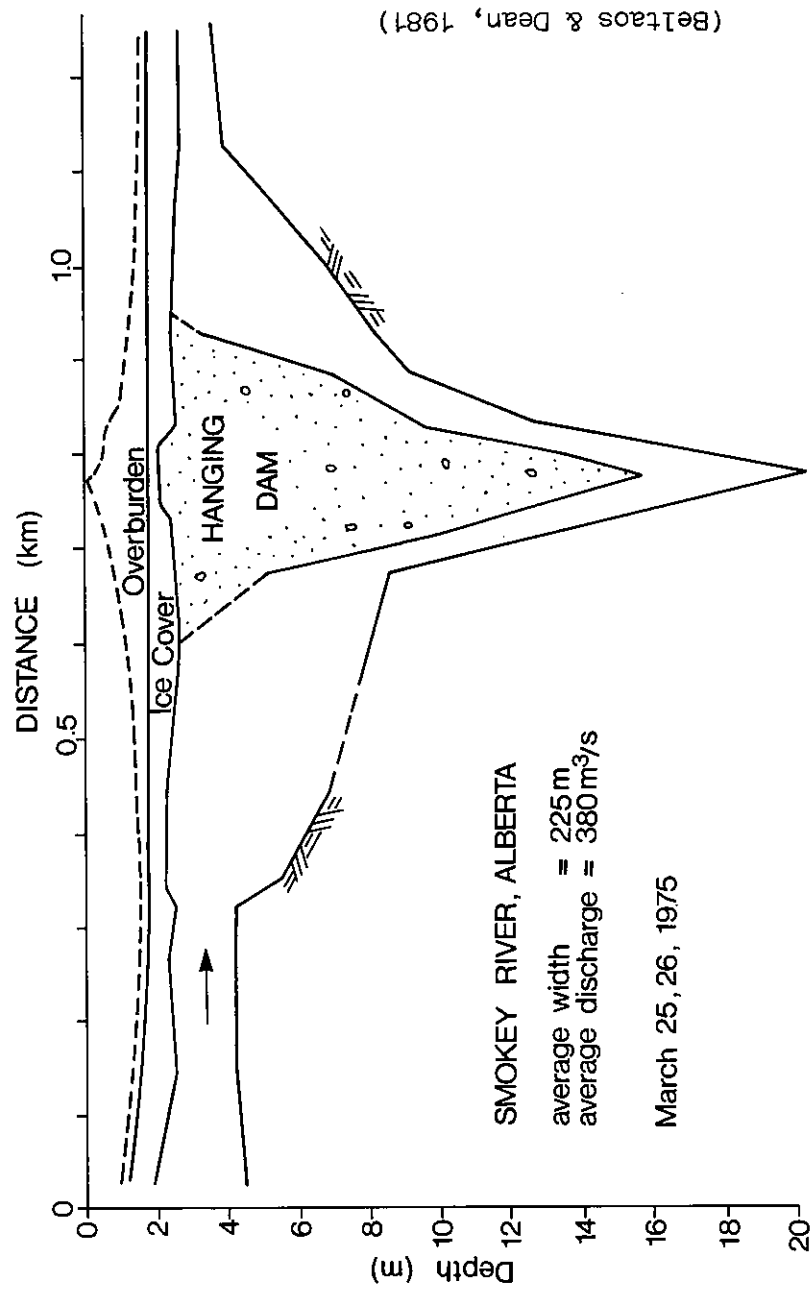


Fig. 14 Example of hanging dam formed at sudden widening and deepening

accumulation will change with time. Nevertheless, some actual figures of these properties as measured from the field will be desirable as they will give some "feel" to one who is faced with frazil accumulation or frazil hanging dam problems.

The dry density, defined as the drained mass of frazil from a frazil/water mixture divided by the volume of the mixture, of the hanging dam shown in Fig. 14 was obtained by Beltaos and Dean (1981) and is shown in Fig. 15. It is seen from Fig. 15 that the dry density of the hanging dam varied from about  $400 \text{ kg/m}^3$  at the lower surface to about  $600 \text{ kg/m}^3$  at a point about 12.5 m above the lower surface. When the measurements were made, the hanging dam was noted to be saturated with water, the frazil crystals had attained the granular form with sizes ranging from 1 mm to 6 mm. Because the density was measured late in the season, the figures shown should represent the upper limit rather than the average values. Using a density of  $920 \text{ kg/m}^3$  for ice, with the above values of dry density, the concentration of frazil ice in the hanging dam can be calculated to vary from 0.43 to 0.65. From the St. Lawrence River with the same methodology, Dean (1977) also found a concentration of 0.50 to 0.60 for the frazil slush deposited under the ice cover.

A note should be added here that the concentrations shown above were not the true concentration of frazil in the frazil accumulation because the drained mass of frazil from the frazil/water mixture is greater than the true mass of frazil, just as the drained mass of sand from a sand/water mixture is greater than the true mass of the sand when dry. However, the information provided by the above researchers can still be useful once the relationship between the drained mass and the true mass of frazil is known. To establish such a relationship should not be too difficult a task.

The shear strength of the hanging dam was also measured by Beltaos and Dean (1981) and the measured values are shown in Fig. 16. From Fig. 16, two points are worth noting. The first is the large fluctuation of the measured strength along a vertical, indicating the large metamorphological and structural variations within a hanging dam, and the second is the tendency of decreasing strength with the reduction in thickness of the frazil accumulation. The latter is understandable as a less accumulation will cause less compaction to the frazil pack and consequently a lower strength.

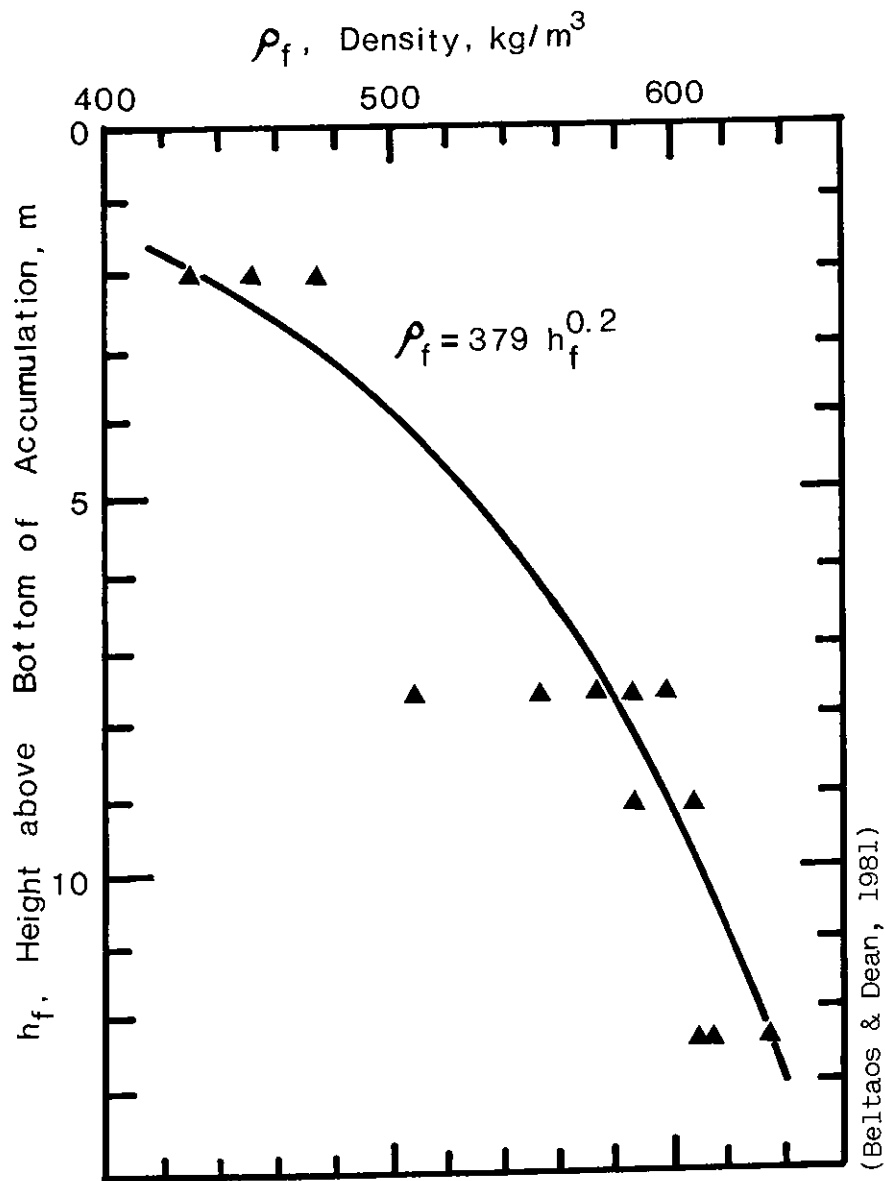


Fig. 15 Dry density of a hanging dam

Beltaos and Dean (1981) also measured the bearing strength of the upper surface of the hanging dam after holes were drilled on the ice cover and the upper surface of the frazil accumulation was exposed to the air. A plate of known dimension was pushed into the pack and the required force when indentation occurred was recorded to calculate the bearing strength. The average bearing strengths for the three verticals shown in Fig. 16 were found to be 300, 150 and 90 kPa ( $10^3 \text{N/m}^2$ ) respectively, in the order of reducing thickness. During the field measurements, large fluctuations of the bearing

strength were also noted. The measured strengths were affected by time and position as well as by the manner in which the measurements were taken.

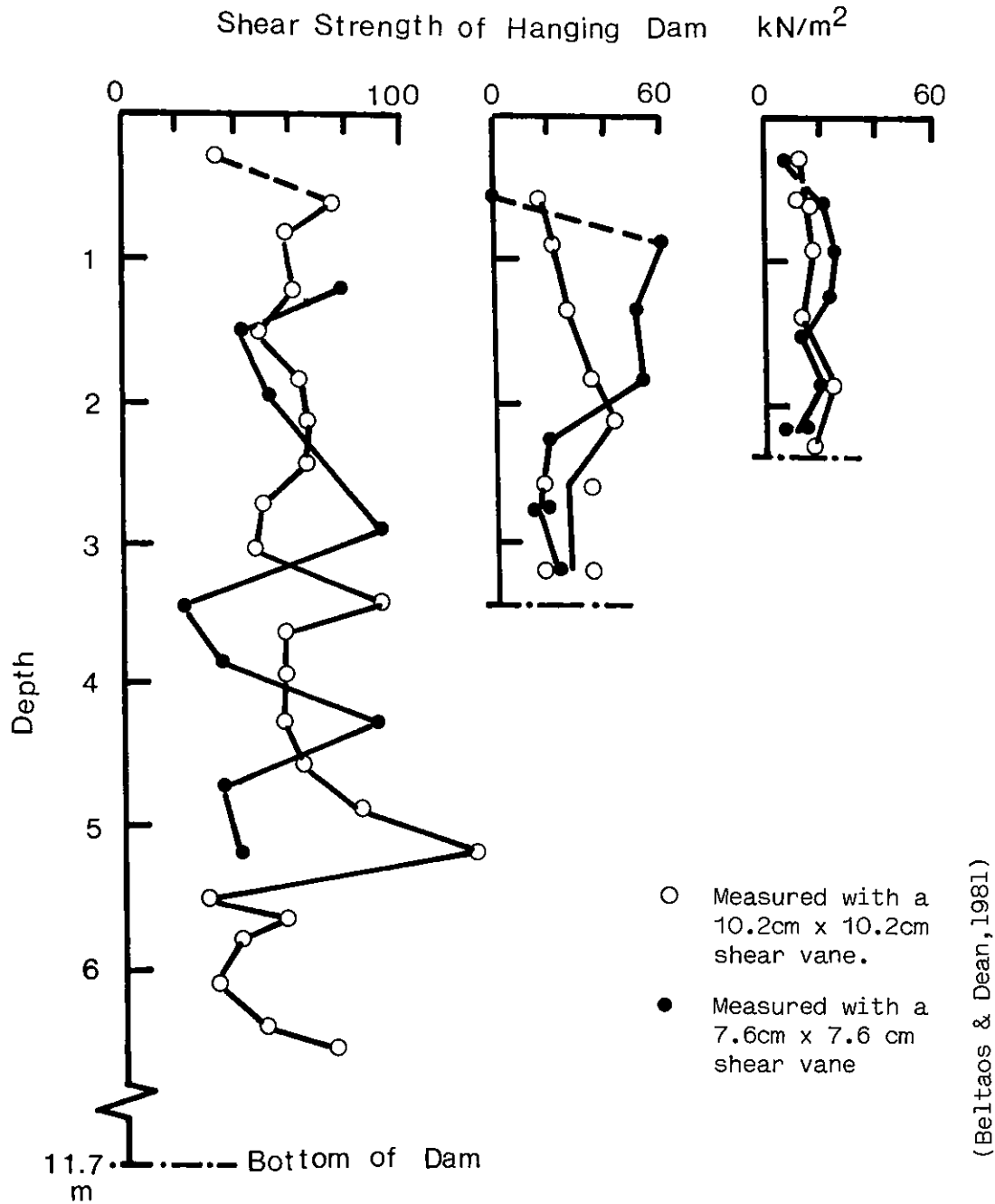


Fig. 16 Shear strength of a hanging dam

#### 5.3.7 Hardening and tunnelling of frazil accumulation

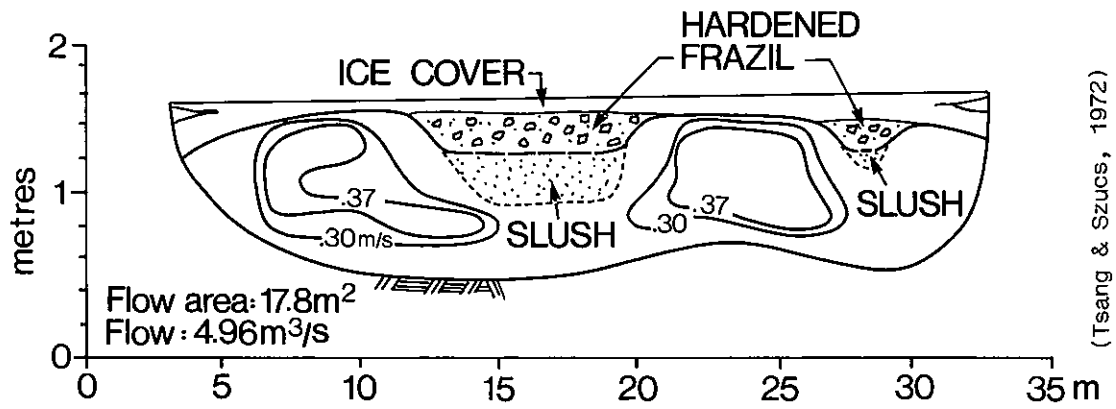
The frazil pack accumulated under the ice cover can be hardened under the action of the flow, the buoyancy of the ice pack and the cold temperature above the ice cover. It is easy to see that the hardening process starts from the upper part and the outer part of the pack. In nature, the hardening of a frazil accumulation is quite common and is known as the "casing" of the frazil ice accumulation. Because of casing, the frazil accumulation can become impervious to the flow and this is known as the "casing effect". However, as time progresses, minute tunnels will start to develop in the pack and gradually increase in size. The casing effect thus is gradually reduced (Bennett, 1968).

It was learned earlier that, once deposited, a frazil pack will not be moved by the flow as dunes, but will be eventually eroded away by the underflow. The deposition, casing, tunnelling and eroding therefore compose the life cycle of a frazil accumulation or a hanging dam. Each stage of the life cycle is greatly affected by the heat fluxes to and from the frazil pack and hence the hydrometeorological conditions.

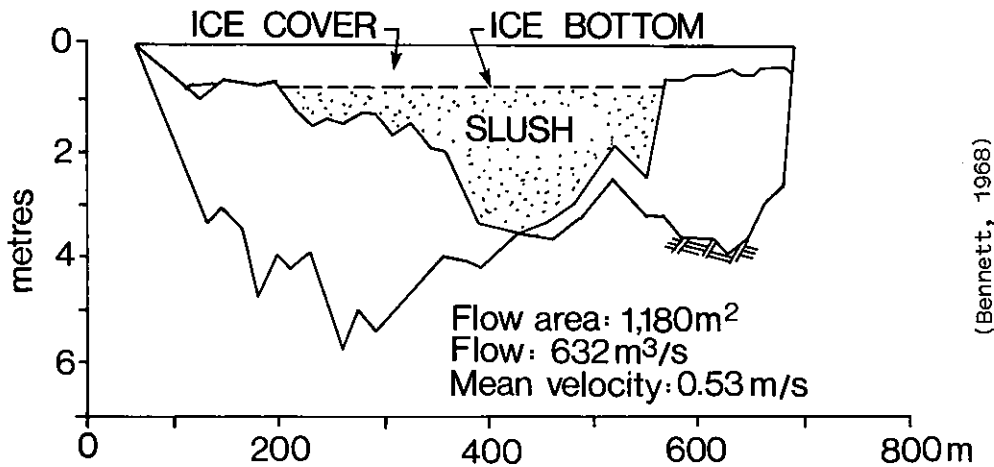
#### 5.4 Effect of Frazil Presence to Velocity Distribution and Frazil Deposition

The presence of frazil affects the velocity distribution of the flow. Field measurements by Tsang (1970) showed that the upper half of the otherwise rather uniform turbulent velocity distribution of a fast ice-covered flow can be modified to an approximately parabolic distribution because of the presence of frazil. Thus, for a cross section of a river, in places where the concentration of frazil is high, a lower flow velocity should be expected. One may view this as the flow being squeezed from the frazil laden part to the frazil free part. Such a property accounts for the accumulation of frazil in the middle of rivers as generally observed in nature. It is known that, in straight reaches of a river, there exists a secondary current in the form of a double vortex, flowing up along the banks and reconverging in the centre of the stream. Such vortex motions transport the frazil to the middle of the river, where now, because of the high concentration of frazil, the flow velocity is reduced to less than the critical velocity so that the frazil can be deposited and accumulate. Figure 17 shows

examples of the deposition of frazil under the ice cover in the middle of the stream for both small and large rivers (Tsang and Szucs, 1972). It is interesting to note the hardened part of the frazil packs shown in Fig. 17a, indicating the progress of the casing process described in the last section.



(a) Nottawasaga River at Alliston, Ontario. Dec.29, 1970.



(b) Peace River at Peace Point, Alberta, Dec.12, 1966.

Fig. 17 Deposition of frazil ice under ice cover



## 6.0 ANCHOR ICE

### 6.1 Turbulence and Its Effects on Cooling of Water and Formation of Frazil

#### 6.1.1 Theory on turbulent diffusion of matters and properties

It has been learned that in rivers and lakes, water is cooled from above. The transport of the chilled water from the surface to the lower layers accounts for the cooling of the water in the lower layers. Before discussing the formation of anchor ice, it will be useful first of all to look at how the supercooled water and frazil are diffused in a turbulent water.

In studying the heat fluxes at the water surface, Eq. 22 was introduced to describe the convection of sensible heat from the water surface to the air. Equation 22, in fact, is applicable for the whole atmosphere. Diffusion equations of such a form, not only are valid for sensible heat transfer but for the transport of other mass-related properties of the turbulence field also. For instance, if one is interested in the flux of temperature, he may write the following equation

$$F_T = -K_T \rho_a (dT/dz) \quad (37)$$

where  $F_T$  is the flux of temperature (or, more precisely, the flux of mass temperature in units of mass degrees/area time) and  $K_T$  is the turbulent diffusion coefficient for temperature.

For a turbulent water body, similar equations, of course, may be written. Thus, for the depression of temperature or the degrees of supercooling, its transport is governed by

$$F_{\Delta T} = -K_{\Delta T} \rho (\partial \Delta T / \partial n) \quad (38)$$

where  $\Delta T$  is the temperature depression or the number of degrees of supercooling,  $n$  is the chosen direction,  $\rho$  is the density of the water,  $K_{\Delta T}$  is the turbulent diffusion coefficient for temperature depression and  $F_{\Delta T}$  is the flux of temperature depression (or, more precisely, the flux of mass-temperature depression). For the transport of frazil ice, the following equation may be written:

$$F_{ci} = -K_{ci} \rho (\partial c_i / \partial n) \quad (39)$$

where  $c_i$  is the concentration of frazil by weight or by volume,  $F_{ci}$  is the flux of frazil ice and  $K_{ci}$  is the turbulent diffusion coefficient for the transport of frazil ice.

According to the theory of turbulent diffusion, the flux of a mass-associated property in a chosen direction is produced by the movement of fluid parcels which bear deviations of the property from the mean from one point to the other along the chosen direction. With such a theory, the flux of temperature depression is expressed by

$$F_{\Delta T} = \overline{\rho v'_n \Delta T'} \quad (40)$$

where  $v'_n$  is the turbulent velocity on the chosen direction and  $\Delta T'$  is the deviation of the temperature depression from the mean. The bar above the expression indicates time-averaged values. In classical theory of turbulence,  $\Delta T'$  is given by

$$\Delta T' = \ell (\partial \overline{\Delta T} / \partial n) \quad (41)$$

where  $\ell$  is a characteristic length specifying the distance over which the fluid parcels moving at the turbulent velocity  $v'_n$  will maintain their own identity. From the above, one sees that for a given temperature-depression distribution, the effectiveness of the turbulence field in diffusing the temperature depression or in diffusing the chilled water from the surface layer to the lower layers depends on the vertical turbulence velocity  $w'$ . The same is also true for the diffusion of frazil to the lower layers.

#### 6.1.2 Turbulent transport of chilled water in lakes and rivers and its effect on frazil formation

Turbulence is generated at the boundaries, either at the surface or at the bottom. As turbulence, itself a property that can be diffused, migrates from the boundaries according to the theory of turbulent diffusion, energy is consumed to overcome viscosity. The turbulence energy in a turbulence field is measured by  $(u'^2 + v'^2 + w'^2)$ , where  $u'$ ,  $v'$  and  $w'$  are turbulence velocity components in the three principal directions respectively. Thus, at a distance sufficiently far away

from the boundary, the turbulence velocity can be reduced to a sufficiently small value that the transport of heat and frazil ice by turbulent diffusion no longer is effectual.

Applying the above discussion to a chilled lake, one sees that the vertical turbulence velocity component  $w'$  will have the maximum value at the surface and diminishes with depth until at a certain depth where it becomes negligible. With such a distribution of  $w'$ , the transport of the chilled water from the surface to the lower layers will be the most effective at the surface and becomes ineffectual at the depth where  $w'$  is small. It follows from the above that, for a deep lake subject to a certain set of meteorological conditions, only the surface layer of a certain thickness can be supercooled and only in that layer can frazil be formed. If the lake is shallow, however, then  $w'$  will not diminish to a negligible value at the bottom and the whole lake is capable of producing frazil. Knowledge of the above has led to the construction of water intakes at sufficient depths in lakes to avoid drawing in frazil.

For a river, when the surface wind drag is negligible, the turbulence is produced at the bottom. As the turbulence migrates upward towards the surface, it diminishes on its way. For a deep river,  $w'$  could be reduced to a negligible value before reaching the surface. In such a case, the chilled water will not be brought down to the lower layers and the ice formed will only be that of static surface ice. On the other hand, if the river is sufficiently shallow so that the value of  $w'$  is still appreciable at the river's surface, then the whole river can be supercooled and capable of producing frazil.

The following is a vivid description of the turbulent mixing of water layers of different temperatures in a river and the production of frazil ice as excerpted from the Ontario Hydro report (1969):

"... Frazil was first detected at the surface when the temperature fell to zero degrees or a trifle less, the water temperature at eight feet depth (just off the river bed) being in the order of  $0.01^{\circ}\text{C}$ . Frazil ice was detected at three feet depth when the temperature at that depth reached  $-0.01^{\circ}\text{C}$ ; the temperature at eight feet depth was  $0^{\circ}\text{C}$ . When the temperature at eight feet depth was reached  $-0.01^{\circ}\text{C}$ , frazil ice was detected near the river bed. Thereafter, the temperature at all depths fell almost to  $-0.02^{\circ}\text{C}$  ..."

The above discussions are for turbulence produced at one boundary only. For situations such as river flow on windy days or lakes with shallow water surface waves, turbulence will be generated both at the surface and at the bottom. Two zones of turbulence thus will result; one expanding from the surface down and the other expanding from the bottom up. If these two zones, meet before  $w'$  in either zone has been reduced to an insignificant value, then the two zones will become one, and effective turbulent diffusion in the whole water body can be expected. Under the above situation, one expects to see a rather uniform temperature distribution as well as a rather uniform frazil ice production in the river or in the lake.

#### 6.1.3 Effect of stratification on turbulent diffusion and frazil formation

Stratification has an important effect on the level and the diffusion of turbulence. It has been mentioned earlier that, when turbulence is diffused from the producing boundary, energy is consumed to overcome viscosity. In the case where there is a stable stratification, more energy will be required to penetrate the stable stratification and this means a thinner turbulence layer and a lower turbulence level. A stable stratification can be produced by surface cooling of the water. It is known that the density of water increases with temperature near the freezing point. Therefore, with a positive temperature gradient in the downward direction for a water body subject to surface cooling, a stable stratification should be expected. The presence of frazil in water also creates a stable stratification. Because of buoyancy, frazil tends to float to the surface. However, turbulence brings some of it back to the lower layers. Thus, at equilibrium, a certain frazil distribution will be established with the concentration of frazil ice decreasing in the downward direction, and accompanying this, a stable stratification. According to the above, one sees that the turbulence level of the chilled water in a lake or a river subject to a given set of hydrometeorological conditions will gradually decrease as the temperature of the water approaches the freezing point, or as the temperature of the water passes  $4^{\circ}\text{C}$ , to be exact. As a consequence, the thickness of the turbulence layer will be reduced. A further reduction of the turbulence level and of the thickness of the turbulence layer should be expected following the formation of frazil ice in the water.

All the above discussions point to the fact that the distribution of temperature and frazil ice in natural rivers and lakes can be complicated. It is even more so if one bears in mind the continual formation of frazil and the diffusion of the latent heat to the surrounding water. Thus, there can be large variations in temperature and frazil concentration in lakes and rivers, both laterally and vertically. Field measurements from Niagara River showed that the lateral temperature variation can be as much as  $0.50^{\circ}\text{C}$  and the vertical temperature variation can be as much as  $0.25^{\circ}\text{C}$ . Only under highly turbulent conditions, will the supercooled water or the frazil crystals be transported to the bottom of the lakes and rivers.

## 6.2 Formation of Anchor Ice

### 6.2.1 Anchor ice formed by underwater nucleation

If the supercooled water can be transported to the bottom, ice may be nucleated on underwater objects to produce anchor ice. Fig. 18a is a picture showing anchor ice grown on a submerged wire (Ontario Hydro, 1970). At the time when the photograph was taken, the water was clear and there was no frazil ice suspended in the water. It is seen from Fig. 18a that the ice coated the wire smoothly and was not in the form of agglomerated ice crystals. More ice was formed on the upstream side of the wire where supercooled water was supplied. Local growths in the form of buds were also noted. As the temperature of the water at the time of formation of the shown anchor ice was only a few hundredths of a degree below  $0^{\circ}\text{C}$ , well above the threshold temperature for heterogeneous nucleation of ice, one may use Michel's theory (1967) to explain the nucleation that on the surface of the river there was a thin layer of highly supercooled water. When the large eddies in the turbulence brought this highly supercooled water in contact with underwater objects, heterogeneous nucleation occurred. Once the primary ice was formed, further ice nucleation took place over the primary ice. Another explanation (Michel, 1980, personal communication) is that ice seeds are produced at the surface. When these ice seeds are transported to the bottom, they nucleate the supercooled water on the underwater objects. Still another conjecture (Hanley, 1980, personal communication) is that ice embryos of subcritical size introduced at the surface may survive the turbulence motion from the top to the bottom, and when these embryos coalesce and become viable embryos, underwater nucleation is initiated. It is

evident that the objects on which anchor ice nucleates need not be on the bottom, as long as they are submerged.

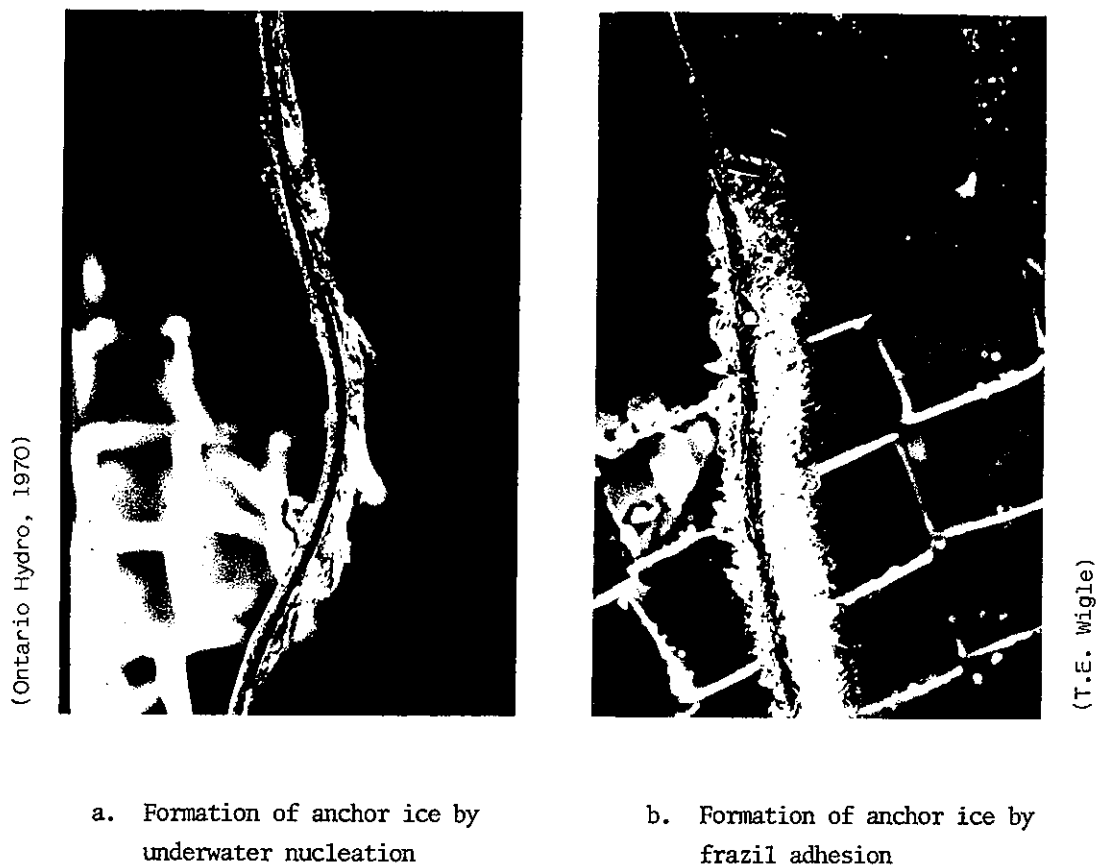


Fig. 18 Formation of anchor ice on underwater objects (Flow from right to left)

#### 6.2.2 Anchor ice formed by frazil adhesion

Besides underwater nucleation, anchor ice can also be formed by frazil ice sticking to underwater objects. It has been mentioned earlier that frazil in supercooled water is very active in that it sticks to underwater objects easily. Thus, in a turbulent flow, if parcels of supercooled water containing frazil ice are transported to the river bottom by turbulence, the frazil will stick to objects on the bottom and produce anchor ice.

Figure 18b (Wigle, 1980, personal communication) is a photograph showing the formation of anchor ice by frazil crystals sticking to an underwater wire and to each other. Comparing Fig. 18a with Fig. 18b, one sees the dramatic

difference in the formation of anchor ice by the two different processes. It is also seen from Fig. 18b that the frazil crystals stuck on their edges rather than on their broad sides. Since, according to crystallography of ice, a frazil crystal grows in supercooled water by adding new ice molecules to its perimeters rather than to its broad faces, the stickiness may be considered as a characteristic of the growing edge of a frazil crystal. Figure 18b again shows that more anchor ice was formed on the upstream side of the wire. The faster growth of anchor ice on the upstream side of the submerged wires should be expected because:

- 1) It was facing the direction of frazil and supercooled water supply, and
- 2) At the upstream side of the wires, the relative velocity between the supercooled flow and the anchor ice was greater than that at the downstream side, or in the wake, of the wire. According to Eq. 31 describing the growth of ice crystals, one can see that the anchor ice on the upstream side of the wires should grow at a faster rate.

It was mentioned earlier (section 4.2) that, before discoid and needle frazil are produced in a river subject to surface cooling, surface flake ice is formed first. The concentration of flake ice is the highest just before the formation of discoid or needle frazil crystals. It was also mentioned that flake ice is active in supercooled water. It follows that, for anchor ice produced by frazil adhesion, the first crystals adhered to underwater objects should be ice flakes. As time progresses and discoid frazil begins to form, the discoid frazil crystals would gradually take over the role of the flake ice and become the main constituents of anchor ice. Such a crystal composition of anchor ice, in fact, is observed in nature as may be seen from Fig. 19. Figure 19 is a photograph of an anchor ice lump formed on the bottom of the Niagara River (Ontario Hydro, 1970; Wigle, 1970). It is seen from the photograph that the lower part or the early part of the lump was composed of large ice platelets and the upper part or the later part was mainly composed of fine frazil crystals. Between these two parts, there was a transitional zone with gradual crystal size changes. The gradual increase in size of the frazil crystals from the top to the bottom of the anchor ice was the result of different degrees of accelerated growth of the frazil crystals. The lower were the frazil crystals, or the earlier they stuck to the anchor ice, the longer time they had in exposing to a higher relative velocity and hence a longer time for accelerated growth. It may be noted that some researchers (Michel, 1980, personal communication) believe that even the flake

ice at the bottom of the anchor ice is a result of the continuous growth of the discoid frazil crystals in the supercooled water.



Fig. 19 Different sizes of crystals forming anchor ice

The stickiness of the frazil ice is an important, but not a necessary condition for the growth of anchor ice, especially at the later stages of anchor ice growth. Because of the petal-like surface of anchor ice, passing ice crystals or platelets can easily be trapped by the rough surface of the anchor ice and this adds to the growth of the anchor ice. The role played by this type of anchor ice growth, of course, is only minor.

It should be noted that anchor ice can be formed by underwater nucleation and by adhesion of active frazil on underwater objects independently. It can also be formed by both processes taking place in concert. In nature, formation of anchor ice by frazil adhesion is the major process.

The two kinds of anchor ice formed by the two different processes have different physical properties. For instance, the anchor ice formed by underwater nucleation is denser and much harder than the anchor ice formed by frazil ice adhesion.

#### 6.2.3 Formation of anchor ice and bottom material

Although in Fig. 18 anchor ice is seen formed over metal wires, the metallic underwater object is not a necessary condition for the formation of



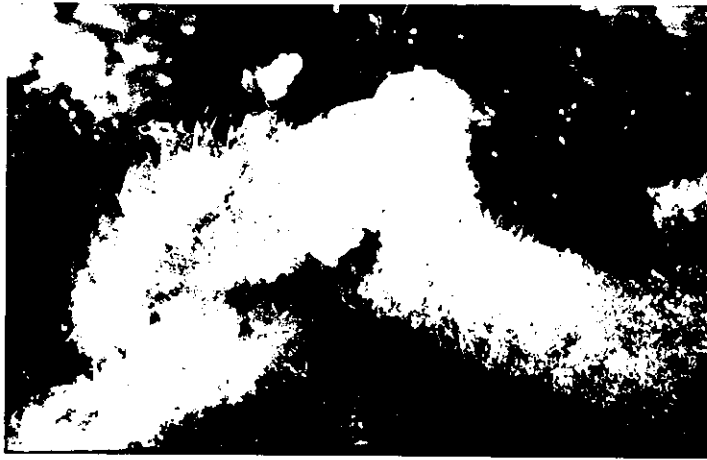
anchor ice. Anchor ice has been observed to form by underwater nucleation and by frazil adhesion on different materials, organic or inorganic. Figure 20 shows examples of anchor ice formation by frazil sticking to different materials. In Fig. 20a (Ontario Hydro, 1968), the formation of anchor ice by frazil sticking to a polypropylene rope is shown. In Fig. 20b (Ontario Hydro, 1969), one sees the formation of anchor ice by frazil sticking to aquatic weeds and in Fig. 20c (Ontario Hydro, 1970; Wigle, 1970), the formation of anchor ice by frazil sticking to a lump of clay is shown. Similar examples on anchor ice formation by direct underwater nucleation on objects of different materials can also be shown.

In spite of the fact that anchor ice can form over different materials, in nature, it is observed that anchor ice forms mostly over boulders, stones, gravels, coarse sands and aquatic weeds, and almost never forms over bottoms of packed fine sand, silt or clay. The reasons for this are not that packed fine sand, silt and clay are ice-phobic as having been proven to be otherwise by Fig. 20c, but the following:

1. Since fine sand, silt and clay particles are small, they can be lifted off the bottom under the buoyancy of the initial anchor ice easily before it can grow to a noticeable size.
2. A compact bottom is more under the influence of the terrestrial heat because it is in the laminar boundary sublayer rather than in the supercooled main stream. Measurements made in the Niagara River showed that at a depth of 10-20 cm below the river bottom, the temperature of the earth was  $0.4-0.5^{\circ}\text{C}$  while the temperature of the flow in the river was below freezing (Ontario Hydro, 1970). Under this geothermal heat, anchor ice would be hard to form except on objects well extended into the supercooled flow. Even if anchor ice could be formed over the bottom, the ice would put a lid to the heat flow and this would eventually lead to a temperature buildup beneath the anchor ice and subsequently a weak bond between the anchor ice and the river bottom. Under the action of buoyancy, the anchor ice would then be lifted off the bottom.

### 6.3 Formation of Anchor Ice in Nature

In the above section, anchor ice is viewed mostly from the microscopic angle. One, however, should not have the misconception that anchor ice only forms a thin layer over underwater objects. Far from it, in nature, anchor ice can grow to large sizes.



(Ontario Hydro, 1968)

a



(Ontario Hydro, 1969)

b



(Ontario Hydro, 1970)

c

Fig. 20 Anchor ice formed on objects of different materials

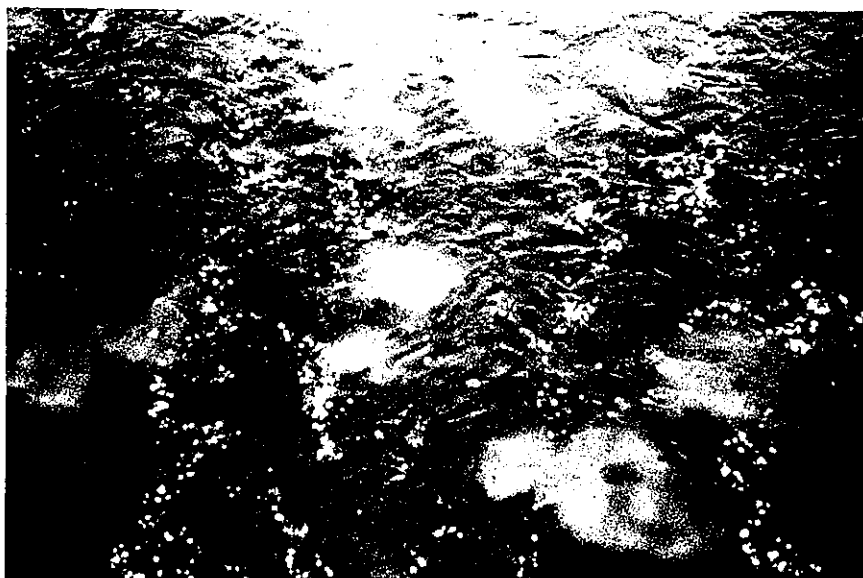
Figure 21a is a picture showing anchor ice formed over boulders as discrete masses. The depth of the water was about 1 m and the size of the anchor ice masses was about 0.5-1 m in diameter. The actual size of the anchor ice masses was larger than that shown in the picture because of the watery colour of the outer part of the anchor ice which made the distinction between water and ice difficult. As the ice masses grow, they will join each other and form a carpet of anchor ice covering the bottom of the rivers as shown in Fig. 21b. For Niagara River, it was found (Ontario Hydro, 1969) that anchor ice can grow to 0.3 to 0.5 m thick against a river depth of about 6 m. For Neva River, 1 m thick anchor ice has been reported against a depth of 20 m (Altberg, 1936).

Anchor ice also contributes to the formation of ice cover on rivers, especially if the anchor ice is formed over large boulders. When the frazil slush and pans drifting with the flow is caught by these anchor ice masses, minute ice covers can be formed. When these minute ice covers grow and join each other, a continuous ice cover is produced.

#### 6.4 Release of Anchor Ice from River Bottom

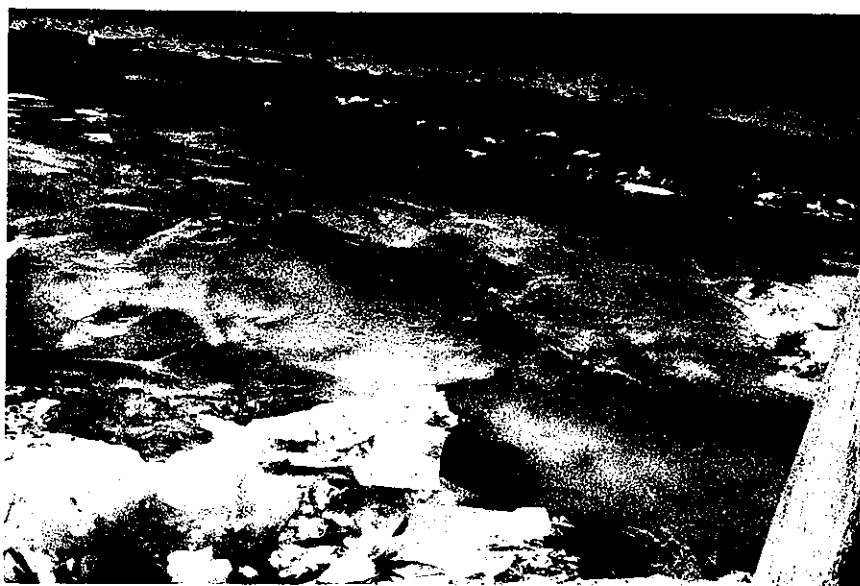
The bond between anchor ice and the river bottom is greatly affected by the heat balance of the water. When anchor ice is first formed, because of the negative heat gain of the water, the bond between the anchor ice and the river bottom is strong. Experiments in the Niagara River showed that under such conditions, the anchor ice would not be dislodged even when the river bottom was raked with an anchor dragged behind an ice breaker. On the other hand, after the bond had been weakened by positive heat gain to the water, the anchor ice could be easily dislodged by the dragged anchor or even by the propeller wash of the ice breaker. As the day progressed and more heat accumulated in the water, the bond between anchor ice and the river bottom could be so weakened that buoyancy alone was sufficient to float the anchor ice off the bottom. For the Niagara River, anchor ice usually is released from the bottom about six hours after the beginning of positive radiation and constitutes the main component of the surface drift ice.

As noted in the last section, anchor ice can be massive, so the buoyant force of the released anchor ice masses can be substantial. It has long been observed that large boulders and heavy anchors can be easily floated up by the released anchor ice (Barns, 1928).



(Beltaos & Tsang)

a



(D. Bray)

b

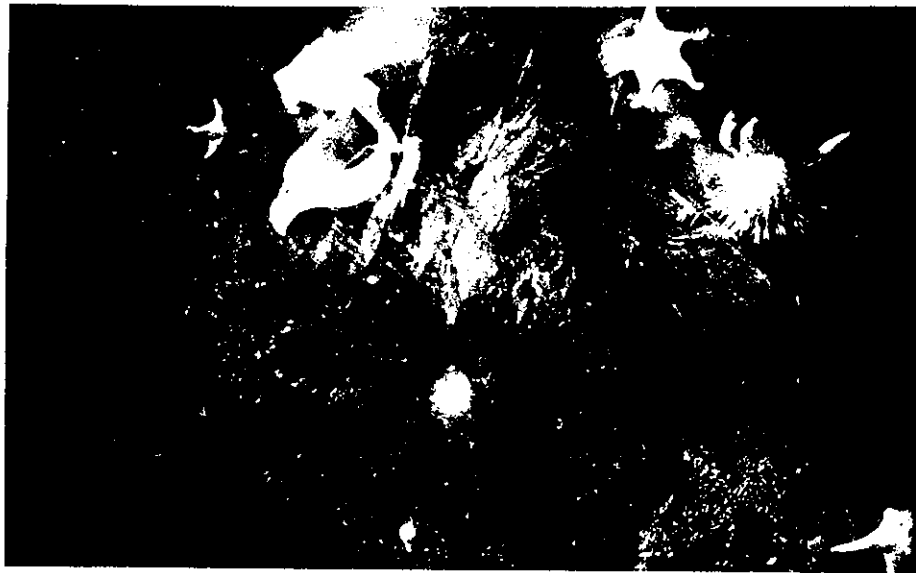
Fig. 21 Anchor ice formed in a natural river

## 6.5 Formation of Anchor Ice in Seawater

As in the case of frazil formation, anchor ice has also been observed to form in the Antarctic under the ice cover (Robilliard, 1980, personal communication). Like freshwater anchor ice, seawater anchor ice can also be formed by direct underwater nucleation or by frazil ice sticking to underwater objects. Figure 22a is a photograph showing an anchor ice mass formed on the Antarctic sea floor by direct ice nucleation. The anchor ice was found in a depth of about 30 m. The nucleation process was so fast that some marine lives were encased by the anchor ice.

Figure 22b is a photograph showing the formation of anchor ice by frazil ice adhesion to a rope. Eventually, the anchor ice around the rope grew into a symmetric, cylindrical mass of about 30-40 cm in diameter as shown in Fig. 22c. Figure 22c was taken after the anchor ice formation process was completed and the rope was lowered from the cut hole in the ice cover for a short length to give a comparison between the size of the rope and the size of the anchor ice. The rope shown in the picture was originally above the water. It is seen from Fig. 22c that the anchor ice tapered gradually down, reflecting a decreasing frazil ice concentration with depth at the time of anchor ice formation. Dayton et al (1969) reported from their Antarctic observations at the same site that the maximum diameter of the anchor ice was at the surface. The diameter decreased with the depth and became zero at a depth of about 33 m.

It is interesting to note that, although the formation of anchor ice by discoid ice crystals and flake ice crystals adhering to underwater objects has been observed (Dayton et al, 1969), the ice crystals forming the anchor ice shown in Fig. 22b were needle crystals. This observed evidence raises the following questions: Is it true that needle frazil is only inactive in freshwater but is active in seawater, or that freshwater needle frazil does not stick to underwater objects because the highly supercooled environment does not exist? Apparently, more research is needed to study the formation of frazil and anchor ice in seawater.



a



b



c

Dark object in centre is  
dirt on lense

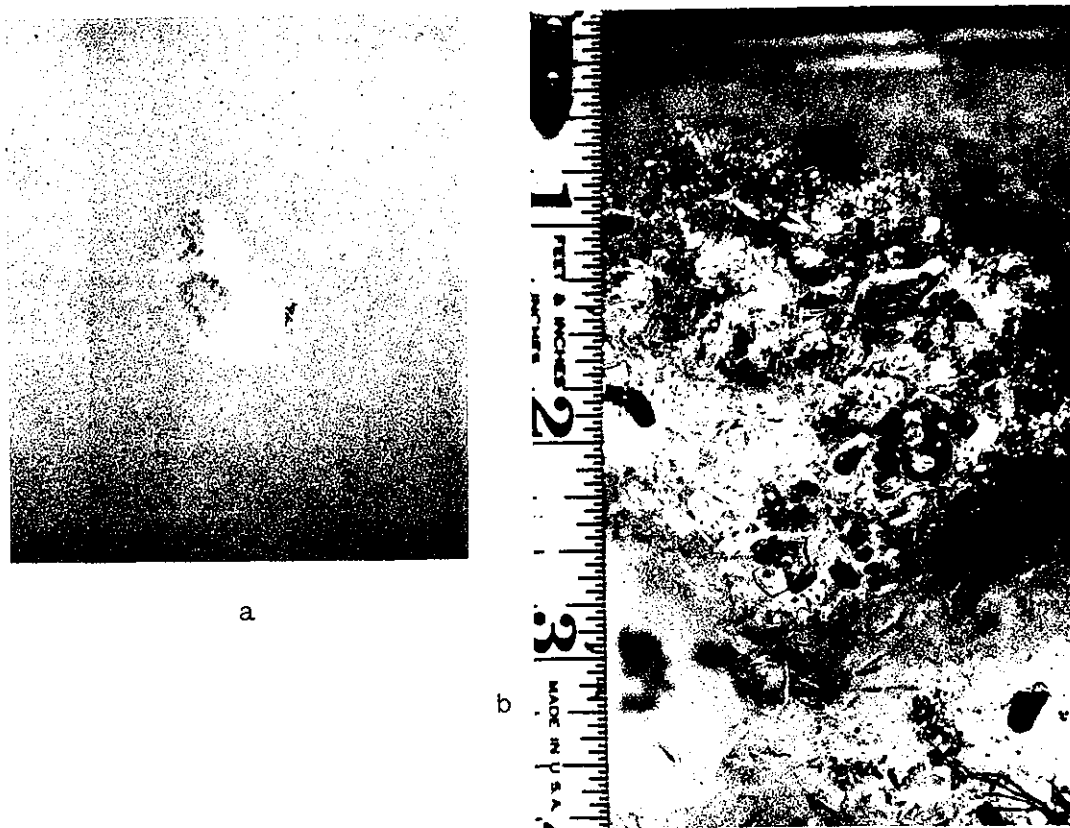
(G.A. Robilliard)

Fig. 22 Anchor ice formed in Antarctic

## 7.0 TRANSPORT OF SEDIMENT AND RESISTANCE EFFECTS OF FRAZIL AND ANCHOR ICE

### 7.1 Transport of Sediment by Frazil and Anchor Ice

Frazil and anchor ice play a role in the transport of sediment in rivers. As frazil crystals agglomerate into clusters and the clusters tumble in the turbulent water, sediment particles are picked up from the river bottom. The sediment particles can either be trapped by the surface of the clusters because of the spongy texture or be stuck to the clusters because of the stickiness of the frazil crystals. The transport of sediment by frazil has been noted by Tsang and Szucs (1972) when they carried out an experimental program on the Nottawasaga River in Southern Ontario. Figure 23 (Ontario Hydro, 1970) contains two photographs showing sediment carrying frazil clusters. In Fig. 23a, fine silt particles were picked up by the cluster. Because silt particles are fine



(Ontario Hydro, 1970)

Fig. 23 Sediment carried by frazil clusters

and light, frazil clusters carrying silt usually remain sufficiently buoyant to be in the suspended state in the water, and float to the surface at places where the turbulence level is low. The cluster shown in Fig. 23a was in the suspended state. The sediment particles picked up by the cluster shown in Fig. 23b were gravel and coarse sand. For frazil clusters incorporating large sediment particles, depending on the weight of the particles, the clusters may remain suspended in the water, bounce or roll along the river bottom, or stay in one place on the river bottom and become points of anchor ice growth. The sediment carried by frazil clusters is redeposited onto the river bottom when the clusters melt or disintegrate.

Anchor ice lifts the sediment particles to which it adheres off the river bottom when the anchor ice has accumulated to a sufficiently large size that the buoyant force produced is greater than the weight of the sediment particles and the cohesive force between the sediment particles. Because anchor ice can accumulate to a great mass, as mentioned in the last chapter, heavy underwater objects can be lifted to the surface by it. Sediment transport by frazil ice and anchor ice, especially the latter, can be quite important for the total sediment activities of a river. For example, for the upper Niagara River which is not a river known for sediment activities in the summer, a considerable quantity of large stones is found added to the downstream end of the river in front of a hydraulic structure each spring. It is thought (Wigle, 1980, personal communication) that only anchor ice can account for the transportation of these large stones. This transport of sediment necessitates frequent dredging of the river.

It is interesting to note that sediment transport by anchor ice can have a profound effect on the ecosystem in lakes and seas of high latitude. For the Antarctic, for instance, it is known that anchor ice can be formed on the sea floor of McMurdo Sound up to a depth of about 33 m (Dayton et al, 1969; Robilliard, 1980, personal communication). Because of this, the seafloor at that particular site at a depth less than 33 m is barren because the anchor ice formed on the seafloor constantly pluck the vegetation and the surface sediment from the seafloor. At a depth greater than 33 m, however, the seafloor all of a sudden changes from a barren zone to a zone of abundant vegetation and, together with it, abundant fauna.



## 7.2 Resistance Effect of Frazil and Anchor Ice

Frazil and anchor ice also affect the resistance of a river. The resistance of a river to flow can be described by the Chezy equation

$$Q = CAR^{1/2}S^{1/2} \quad (42)$$

where  $Q$  is the rate of discharge,  $A$  is the cross-sectional area of the flow  $S$  is the surface slope of the river,  $R$  is the hydraulic radius and is defined as  $A/P$ ,  $P$  being the wetted perimeter and  $C$  is known as the Chezy discharge coefficient. Besides the Chezy equation, the resistance of a river may also be described by either the Manning equation or the Darcy-Weisbach equation.

In studying the resistance of ice-covered rivers, the usual way is to divide the flow into the upper and the lower flow layers, to evaluate the resistance coefficients of the ice cover and the river bed separately first and then calculate the composite resistance coefficient of the whole flow according to different theoretical models. In the study by Tsang (1980, 1982), however, the flow was treated as a whole and the hydraulic radius was calculated as if ice did not exist. A corrective coefficient  $\phi$  was introduced to the right hand side of the Chezy equation to take into account the ice effect. For a river flowing under summer and winter conditions with the same surface slope and the same flow area, it is seen from Eq. 42 that  $\phi$  means the ratio of winter flow to summer flow.

Figure 24 is a plotting of  $\phi$  versus time for the Beauharnois Canal, a man-made channel carrying the discharge in the St. Lawrence River to a power station near Montreal. In the diagram, the fractional ice cover is also shown. The plots are based on the 1972-73 winter field data. The Chezy's  $C$  value of Beauharnois Canal is approximately  $40 \text{ m}^{1/2}/\text{s}$  under summer flow conditions. It is seen from Fig. 24 that two days after ice appearance on the river, although the river was only about eight percent ice covered, the value of  $\phi$  has been reduced to a value of about 0.61 from unity. The ice in the Beauharnois Canal for the first few days of the ice season is mostly in the form of slush ice. Thus, one sees from Fig. 24 that the presence of frazil slush in a river can reduce the carrying capacity of the river by as much as 40 percent. The reason that such a reduction was caused by frazil presence and not by the partial ice cover can be seen from

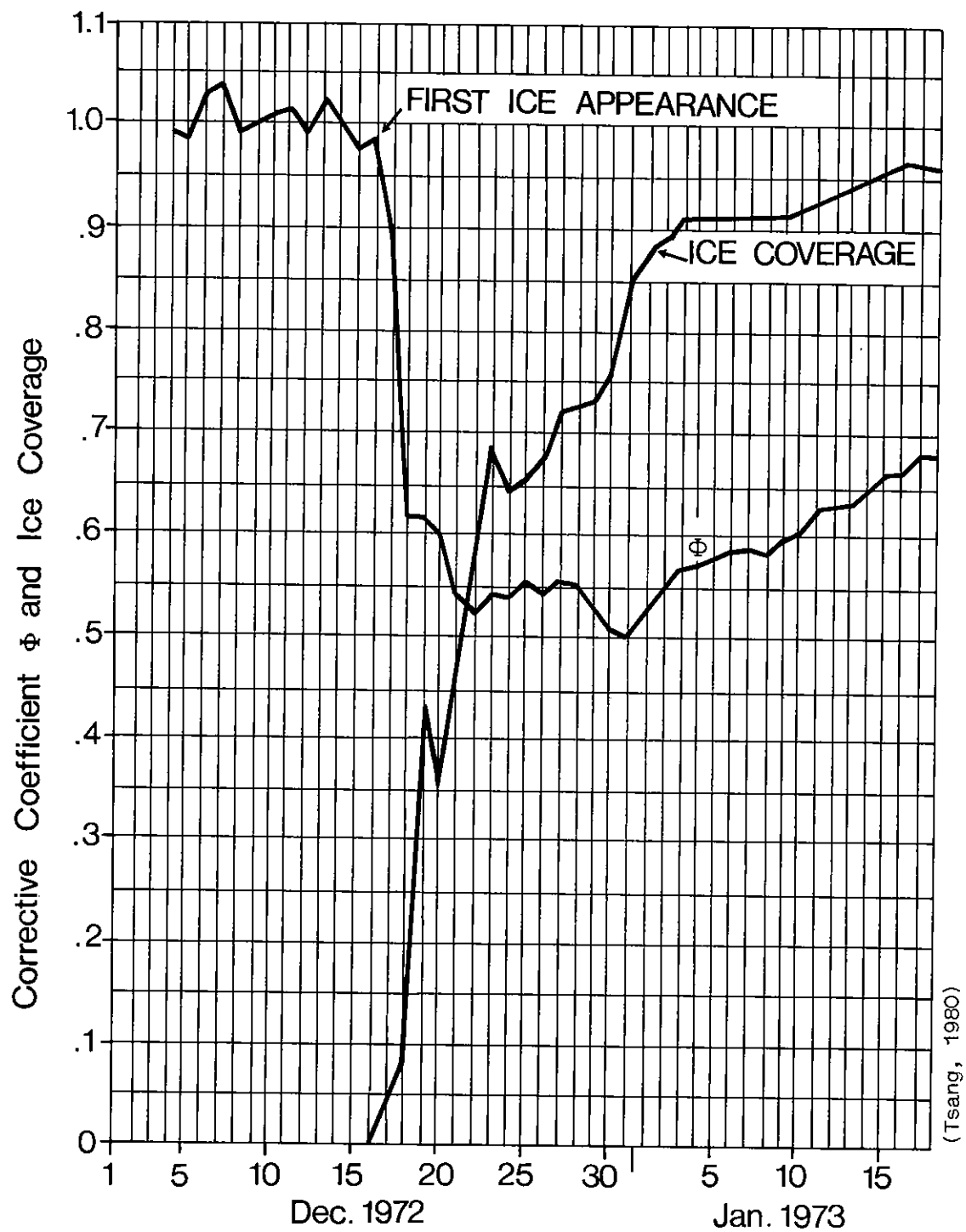


Fig. 24 Corective coefficient of Beauharnois Canal

the fact that on the third day after first ice appearance in the river, although the percentage of ice cover of the river has been increased to 44 percent, no change was effected on the corrective coefficient  $\phi$ .

The modification of resistance of a river to flow because of anchor ice presence has not yet been systematically studied. However, for the upper Niagara River, which has a summer Chezy's coefficient of  $C=61 \text{ m}^{1/2}/\text{s}$ , operational records (Ontario Hydro, 1969) show that the formation of anchor ice in the river can cause a reduction in discharge by as much as  $1400 \text{ m}^3/\text{s}$  against a total discharge of  $5600 \text{ m}^3/\text{s}$ , representing a flow reduction of 25 percent. Such a reduction in the discharge can take place within four hours. Since, for the upper Niagara River, the upstream water level and downstream water level both vary little, being the surface of a large water body and in front of a control, the above reduction in discharge means a corrective coefficient as small as 0.75.

When both frazil and anchor ice are present in the flow, an even smaller corrective coefficient could be expected. Unfortunately, resistances of rivers under both frazil and anchor ice conditions have not been systematically documented. Foulds and Wigle (1977) reported a 30 percent reduction of flow in three hours because of frazil and anchor ice formation in a river. Should all the hydraulic parameters remain unchanged, this would represent a corrective coefficient of about 0.7. The change in flow because of the formation of frazil and anchor ice in a small stream of a discharge of the order of  $1 \text{ m}^3/\text{s}$  was studied by Gilfilian et al (1972). Based on their measured data, the Chezy C under summer conditions can be calculated to be  $33.3 \text{ m}^{1/2}/\text{s}$  and the corrective coefficient can be calculated to be 0.7. This resistance condition occurred when 16 percent of the water was changed into ice. However, the percentage distribution of frazil, anchor ice and border ice was not known. Based on the above researchers' works, one probably can say that a corrective coefficient of 0.7 is quite in order for a large or a small river producing frazil and anchor ice.

### 7.3 Resistance Effect of Hanging Dams

It was shown above that the presence of frazil ice in an open flow can greatly increase the resistance of the river. The same is also true for the formation of a hanging dam in an ice-covered flow. It is seen from Eq. 42 that the resistance of a river can be described by the value of its Chezy's coefficient C. Besides C, the resistance of a river can also be described by the Manning roughness coefficient  $n$  which is defined by

$$Q = \frac{1}{n} A R^{2/3} S^{1/2} \quad (43)$$

Using the La Grande River hanging dam data, Michel and Drouin (1974) found that the composite Manning  $n$  value for the ice-covered flow with the hanging dam shown in Fig. 10 was 0.063.

As mentioned earlier, the composite Manning's  $n$  of an ice covered-river can be calculated from the Manning's  $n$  of the ice cover and the river bed employing different formulae. One of the most popular formulae is the Sabanev formula which is as follows:

$$n = \left( \frac{n_1^{3/2} + n_2^{3/2}}{2} \right)^{2/3} \quad (44)$$

where the subscripts 1 and 2 refer to the ice cover and the river bed respectively. Using the above equation, from the measured composite Manning's  $n$  of 0.063 and a river bed Manning's  $n$  value of 0.028 derived from summer flow, Michel and Drouin obtained a Manning's  $n$  value of  $n_1=0.080$  for the ice cover with the hanging dam in the La Grande River and considered it typical for a hanging dam.

While measuring the accumulated frazil ice under the ice cover in the International Rapids section of the St. Lawrence River in mid and late winter, Dean (1977) reported the rate of discharge and the head difference across the section under ice-covered conditions, with and without frazil accumulation. From his data, one can calculate the corrective coefficient for the Chezy  $C$  of the ice-covered flow with a frazil deposition of a thickness of 20-30 percent the total depth to be  $\phi_f=0.68 \phi_i$ , where  $\phi_i$  is the corrective coefficient for the ice-covered flow without frazil deposition. In studying the winter flow in the Beauharnois Canal, Tsang (1980, 1982) found that in mid and late winter,  $\phi_i$  could be as low as around 0.8. Using this value, the corrective coefficient for the ice-covered flow with frazil deposition can be calculated to be as small as 0.54. In other words, in mid and late winter an ice-covered river with frazil accumulation under the ice cover will, under otherwise identical conditions, only carry about half of its summer flow. This conclusion is also supported by Fig. 24. It is seen from Fig. 24 that, at the end of December 1972, the Beauharnois Canal was about 80 percent ice covered and the corrective coefficient was about 0.5. Since it has been noted earlier that, prior to this time, there was an abundance of frazil ice in the river, the small corrective coefficient value of 0.5 thus could be produced by the ice cover plus the frazil deposition.

It is seen from the preceeding chapters that, although frazil and anchor ice have been there since the beginning of humanity, they are not well understood to this day. This monograph can only be considered as an initial attempt in presenting the present state of the knowledge in a self-contained, comprehensive text. As our knowledge of frazil and anchor ice expands, this monograph will have to be periodically updated, expanded and modified.

A major road block to the advancement of our knowledge on frazil and anchor ice has been the lack of a working instrument that can quantitatively measure frazil and anchor ice. Although some attempt has been made to produce an instrument that can measure the concentration of frazil and experimental models have been constructed (Kristinsson, 1970; Schmidt and Glover, 1975; Tsang, 1977), it will still be some time before a reliable and manufacturable instrument is available in the market. For anchor ice, no attempt is known in the published literature to develop an instrument for its measurement. The high cost and inherent danger of conducting field programs during the time of frazil and anchor ice production post other research problems. Although some aspects of the research can be conducted in the laboratory, such laboratories usually require refrigeration and consequently high capital investment. The main reason for the slow progress in frazil and anchor ice research probably is that the topics had not been socially considered as important enough. How many of us knew there were such things as frazil and anchor ice in our school years and, in fact, in our undergraduate years ?

The needed social attention, however, has been received following the recent energy crisis and the development of northern energy resources. This has led to relatively fast advancement of our knowledge of the topics in the past decade and more research efforts are being made today. Thus, one may enthusiastically look forward to a well improved state of the science in the near future.

One chapter that ought to but has not been included in this monograph is the engineering aspects of frazil and anchor ice. What are the practical problems that are caused by them and how do we counteract these problems? There must be a rich pool of information on this subject. However, such information is likely in its raw and fragmented form. Great effort will be

needed to extract the relevant information from the available raw material for writing a chapter on frazil and anchor ice engineering. It is hoped that in the next edition of the monograph such a chapter will be included.

## REFERENCES

- Altberg, W. J., 1936. "Twenty Years of Work in the Domain of Underwater Ice Formation (1915-1935)". Bulletin No. 23, International Association of Scientific Hydrology, pp. 373-407.
- Altberg, W. J., 1938. "On the Centres or Nuclei of Water Crystallization" - "O Tsentrah ili Iadrakh Frystallizatsii Vody". Meteorologiya i Gidrologiya, Bulletin No. 3, pp. 3-12, DLC, QC851.M27. CRREL Translation TL 294, January 1972.
- Anderson, E. R., 1954. "Energy Budget Studies, in Water Loss Investigation: Lake Hefner Studies". Technical Report, U.S. Geological Survey Professional Paper 269, pp. 71-118.
- Arakawa, K., 1954. "Experimental Studies on Freezing of Water". Publication No. 39, International Association of Scientific Hydrology, pp. 474-477.
- Arakawa, K., 1954. "Studies on the Freezing of Water (II) - Formation of Disc Crystals". Journal of the Faculty of Science, Hokkaido University, Japan, Series II, Vol. IV, No. 5, pp. 311-339
- Arakawa, K., 1967. "The Growth of Ice Crystals in Water". Proceedings of International Conference on Low Temperature Sciences, Hokkaido University, Sapporo, Japan, pp. 463-464.
- Arden, R. S. and Wigle, T. E., 1972. "Dynamics of Ice Formation in the Upper Niagara River". Proceedings of Banff Symposia on the Role of Snow and Ice in Hydrology, Unesco-WMO-IAHS, Banff, September, Vol. 2, pp. 1296-1312.
- Asvall, R. P., 1972. "Change in Ice Conditions in Regulated River Basins". Proceedings of Banff Symposia on the Role of Snow and Ice in Hydrology, Banff, September, Vol. 2, pp. 1283-1295.
- Barnes, H. T., 1928. "Ice Engineering." Renouf Publishing Co., Montreal.
- Beltaos, S. and Dean, A. M. Jr., 1981. "Field Investigations of a Hanging Ice Dam". Proceedings of IAHR International Symposium on Ice, Quebec, July.
- Bennett, R. M., 1968. "The Stage-Discharge Relationship under Ice Cover for the Peace and Slave Rivers". M. Sc. Thesis, Utah State University.
- Carstens, T., 1966. "Experiments with Supercooling and Ice Formation in Flowing Water". Geofysiske Publikasjoner, Vol. 26, No. 9, pp. 1-18.
- Carstens, T., 1970. "Heat Exchange and Frazil Formation". Proceedings of IAHR Symposium on Ice and Its Action on Hydraulic Structures, September, Reyjavik, paper 2.11.

- Cousineau, E., 1959. "Some Aspects of Ice Problems Connected with Hydro-electric Developments". Engineering Journal, Vol. 42, No. 3, pp. 48-54.
- Dayton, P. K, Robilliard, G. A. and DeVries, A. L., 1969. "Anchor Ice Formation in McMurdo Sound, Antarctica and Its Biological Effects". Science, Vol. 163, January, pp. 273-274.
- Dean, A. M. JR., 1977. "Remote Sensing of Frazil and Brash Ice". 3rd National Hydrotechnical Conference, Quebec, May, pp. 693-704.
- Devik, O., 1931. "Thermische und dynamische bedingungen der eisbildung im Wasserlaufen". Geofys. Publ. IX, 1.
- Devik, O., 1944. "Ice Formation in Lakes and Rivers". The Geographical Journal, V. CIII, No. 5, May, pp. 193-203.
- Dingman, S. L., Weeks, W. F. and Yen, Y. C., 1968. "The Effect of Thermal Pollution on River Ice Conditions". Water Resources Research, Vol. 4, No. 2, April, pp. 349-362.
- Ferguson, H. L. and Cork, H. F., 1972. "Regression Equations Relating Ice Conditions in the Upper Niagara River to Meteorological Variable". Proceedings of Banff Symposia on the Role of Snow and Ice in Hydrology, Banff, September, pp. 1314-1326.
- Fernandez, R. and Barduhn, A. J., 1967. "The Growth Rate of Ice Crystals". Desalination, Vol. 3, 1967, pp. 330-342.
- Foulds, D. M. and Wigle, T. E., 1977. "Frazil - The Invisible Strangler". Journal of Americal Water Works Association, April, pp. 196-199.
- Gilfilian, R. E., Kline, W. L., Osterkamp, T. E. and Benson, C. S., 1972. "Ice Formation in a Small Alaskan Stream". Proceedings of Banff Symposia on the Role of Snow and Ice in Hydrology, September, Banff, pp. 505-513.
- Hanley, T. O'D., 1978. "Frazil Nucleation Mechanisms". Journal of Glaciology, Vol. 21, No. 85, pp. 581-587.
- Hanley, T. O'D., and Michel, B., 1977. "Laboratory Formation of Border Ice and Frazil Slush". Canadian Journal of Civil Engineering, Vol. 4, No. 2, pp. 153-160.
- Hanley, T. O'D. and Rao, S. R., 1980. "Acoustic Detection of Frazil Formation". Proceedings of Workshop on Hydraulics Resistance of River Ice, National Water Research Institute, Environment Canada, Burlington, Ontario, September, pp. 238-241.
- Kivisild, H. R., 1970. "River and Lake Ice Terminology". Proceedings of IAHR Symposium on Ice and Its Action on Hydraulic Structures, Iceland, Paper 1.0.



- Kivisild, H. R., 1959. "Hydrodynamic Analysis of Ice Floods". Proceedings of IAHR, 8th Congress, Montreal.
- Kristinsson, B., 1970. "Ice Monitoring Equipment". Proceedings of Symposium on Ice and Its Action on Hydraulic Structures, IAHR, Sept., Reyjavik, pp. 1.1, 1-14.
- \* Lathem, K. W. "Ice Regime Investigations on the Moira River at Belleville, Ontario". Proceedings Research Seminar on Thermal Regime of River Ice, October 1974, Quebec. NRC Technical Memorandum No. 114, Ottawa, January 1975, pp. 109-120.
- List, R. J., 1968. "Smithsonian Meteorological Tables". Smithsonian Institute Publication, 6th ed.
- List, R. and Barrie, L. A., 1972. "Heat Losses and Synoptic Patterns Relating to Frazil Ice Production in the Niagara River". Proceedings Banff Symposia on the Role of Snow and Ice in Hydrology, September, pp. 1328-1338.
- Mason, B. J., 1958. "The Supercooling and Nucleation of Water". Advances in Physics, Vol. 7.
- Michel, B., 1967. "Morphology of Frazil Ice". Proceedings of International Conference on Low Temperature Science, Hokkaido University, Sapporo, Japan, pp. 119-128.
- Michel, B., 1967. "From the Nucleation of Ice Crystals In Cloud to the Formation of Frazil Ice in Rivers". Proceedings of International Conference on Low Temperature Science, Hokkaido University, Sapporo, Japan, pp. 129-136.
- Michel, B., 1972. "Properties and Processes of River and Lake Ice". Proceedings of Banff Symposia on the Role of Snow and Ice in Hydrology, September, Banff, pp. 454-481.
- \* Michel, B., 1978. "Ice Mechanics". Les Presses de L'Universite, Laval, Quebec.
- Michel, B. and Drouin, M., 1974. "Equilibrium of an Underhanging Dam at the La Grande River". Unpublished Manuscript Intended for River and Ice Symposium, Budapest, January.
- Ontario Hydro, 1967. "Study of River and Lake Ice - I.H.D. Project No. R-SIG-6 Ontario-27". Progress Report No. 1, Niagara River Ice, June, Contributors: Bryce, J. B., Arden, R. S., Wigle, T. E. and Foulds, D. M..
- Ontario Hydro, 1968. "Study of River and Lake Ice - I.H.D. Project No. C.6.7, File Reference: R-SIG-6; Ontario 27". Progress Report No. 2, Niagara River Ice, June, Contributors: Bryce, J. B., Arden, R. S., Wigle, T. E. and Foulds, D. M..

- Ontario Hydro, 1969. "Study of River and Lake Ice - I.H.D. Project No. C.6.7, File Reference: R-SIG-6; Ontario-27". Progress Report No. 3, Niagara River Ice, September, Contributors: Bryce, J. B., Arden, R. S. and Wigle, T. E..
- Ontario Hydro, 1970. "Study of River and Lake Ice - I.H.D. Project No. C.6.7, File Reference: R-SIG-6; Ontario-27". Progress Report No. 4, Niagara River Ice, December, Contributors: Bryce, J. B., Arden, R. S. and Wigle, T. E..
- Osterkamp, T. E., 1978. "Frazil Ice Nucleation Mechanisms". Scientific Report, Geophysical Institute, University of Alaska, February, 13 p.
- Osterkamp, T. E., 1978. "Frazil Ice Formation: A Review". Journal of the Hydraulics Division, ASCE, September, pp. 1239-1255.
- Rimsha, V. A. and Donchenko, R. V., 1957. "The Investigation of Heat Loss from Free Water Surfaces in Winter Time". (In Russian), Trudy Leningrad, Gosud. Hidrol. Inst., 65, pp. 54-83.
- Schmidt, C. D. and Glover, J. R., 1975. "A Frazil Ice Concentration Measuring System Using a Laser Doppler Velocimeter". Journal of Hydraulic Research, IAHR, Vol. 13, No. 3, pp. 299-314.
- Tsang, G., 1970. "Change of Velocity Distribution in a Cross Section of a Freezing River and the Effect of Frazil Ice Loading on Velocity Distribution". Proceedings of IAHR Symposium on Ice and Its Action on Hydraulic Structures, September, Reykjavik, pp. 3.2.1-3.2.11.
- Tsang, G., 1977. "Development of an Experimental Frazil Ice Instrument". Proceedings of 3rd National Hydrotechnical Conference, CSCE, Quebec, May, pp. 671-692.
- Tsang, G., 1980. "Resistance of Beauharnois Canal in Winter". Workshop on Hydraulic Resistance of River Ice, Proceedings, September, Burlington, pp. 57-78. Also, 1982, Journal of the Hydraulics Division, ASCE, in press.
- \* Tsang, G. and Szucs, L., 1972. "Field Experiments of Winter Flow in Natural Rivers". Proceedings of International Symposia on the Role of Snow and Ice in Hydrology, Banff, September, pp. 772-796.
- Wigle, T. E., 1970. "Investigations into Frazil, Bottom Ice and Surface Ice Formation in the Niagara River". Proceedings of IAHR Symposium On Ice and Its Action on Hydraulic Structures, September, Reyjavik, Paper 2.8.

Williams, G. P., 1972. "A Case History of Forecasting Frazil Ice". Proceedings of the Banff Symposia on the Role of Snow and Ice in Hydrology, Unesco-WHO-IAHS, September, Vol. 2, pp. 1212-1223.

## APPENDIX - Tables of Conversion

The following tables of conversion are given for easy conversion between different unit systems:

### Temperature

	<u>°K</u>	<u>°C</u>	<u>°F</u>
°K	= 1	°C + 273.15	$\frac{5}{9} (°F + 459.67)$
°C	= °K - 273.15	= 1	$\frac{5}{9} (°F - 32)$
°F	= $1.8(°K - 459.67)$	$1.8°C + 32$	= 1

### Pressure

	<u>Pa=1 N/m<sup>2</sup></u>	<u>atm</u>	<u>bar</u>	<u>kgf/m<sup>2</sup></u>	<u>lbf/in<sup>2</sup></u>
1 Pa	= 1	$9.869 \times 10^{-6}$	$10^{-5}$	$1.02 \times 10^{-1}$	$1.45 \times 10^{-4}$
1 atm	= $1.013 \times 10^5$	= 1	1.013	$1.03 \times 10^4$	14.70
1 bar	= $10^5$	$9.869 \times 10^{-1}$	= 1	$1.02 \times 10^4$	14.50
1 kgf/m <sup>2</sup>	= 9.806	$9.678 \times 10^{-5}$	$9.806 \times 10^{-5}$	= 1	$1.422 \times 10^{-3}$
1 lbf/in <sup>2</sup>	= $6.894 \times 10^3$	$6.804 \times 10^{-2}$	$6.894 \times 10^{-2}$	$7.031 \times 10^2$	= 1
1 millibar = $10^{-3}$ bar					

### Heat

	<u>J</u>	<u>Wh</u>	<u>Cal</u>	<u>Btu</u>	<u>erg</u>
1 J	= 1	$2.778 \times 10^{-4}$	$2.388 \times 10^{-1}$	$9.478 \times 10^{-4}$	$10^7$
1 Wh	= $3.6 \times 10^3$	= 1	$8.598 \times 10^2$	3.412	$3.6 \times 10^{10}$
1 Cal	= 4.187	$1.163 \times 10^{-3}$	= 1	$3.968 \times 10^{-3}$	$4.187 \times 10^7$
1 erg	= $10^{-7}$	$2.778 \times 10^{-11}$	$2.389 \times 10^{-8}$	$9.478 \times 10^{-11}$	= 1

### Latent Heat

	<u>J/Kg</u>	<u>Cal/g</u>	<u>Btu/lb</u>
1 J/Kg	= 1	$2.389 \times 10^{-4}$	$4.299 \times 10^{-4}$
1 Cal/g	= $4.187 \times 10^3$	= 1	1.8
1 Btu/lb	= $2.326 \times 10^3$	$5.555 \times 10^{-1}$	= 1

### Specific Heat

	<u>J/Kg<sup>o</sup>C</u>	<u>Cal/g<sup>o</sup>C</u>	<u>Btu/lb<sup>o</sup>F</u>
1 J/Kg <sup>o</sup> C =	1	$2.389 \times 10^{-4}$	$2.389 \times 10^{-4}$
1 Cal/g <sup>o</sup> C =	$4.187 \times 10^3$	1	1
1 Btu/lb <sup>o</sup> F =	$4.187 \times 10^3$	1	1

### Intensity of Heat Flow Rate (Heat Flux)

	<u>W/m<sup>2</sup></u>	<u>Cal/cm<sup>2</sup>h</u>	<u>Btu/ft<sup>2</sup>h</u>
1 W/m <sup>2</sup> =	1	$8.598 \times 10^{-2}$	$3.170 \times 10^{-1}$
1 Cal/cm <sup>2</sup> h =	$1.163 \times 10^1$	1	3.687
1 Btu/ft <sup>2</sup> h =	3.155	$2.713 \times 10^{-1}$	1

### Length

	<u>m</u>	<u>cm</u>	<u>ft</u>	<u>in</u>
1 m =	1	$10^2$	3.280	39.370
1 cm =	$10^{-2}$	1	$3.280 \times 10^{-2}$	$39.370 \times 10^{-2}$
1 ft =	$3.048 \times 10^{-1}$	$3.048 \times 10^1$	1	12
1 in =	$2.540 \times 10^{-2}$	2.540	$8.333 \times 10^{-2}$	1

### Velocity

	<u>m/s</u>	<u>cm/s</u>	<u>ft/s</u>	<u>in/s</u>
1 m/s =	1	$10^2$	3.280	39.370
1 cm/s =	$10^{-2}$	1	$3.280 \times 10^{-2}$	$39.370 \times 10^{-2}$
1 ft/s =	$3.048 \times 10^{-1}$	$3.048 \times 10^1$	1	12
1 in/s =	$2.540 \times 10^{-2}$	2.540	$8.333 \times 10^{-2}$	1

### Discharge

	<u>m<sup>3</sup>/s</u>	<u>ft<sup>3</sup>/s</u>	<u>litre/s</u>
1 m <sup>3</sup> /s =	1	$3.531 \times 10^1$	$10^3$
1 ft <sup>3</sup> /s =	$2.832 \times 10^{-2}$	1	$2.832 \times 10^1$
1 litre/s =	$10^{-3}$	$3.531 \times 10^{-2}$	1

### Density

	<u>Kg/m<sup>3</sup></u>	<u>g/cm<sup>3</sup></u>	<u>slug/ft<sup>3</sup></u>
1 Kg/m <sup>3</sup>	= 1	10 <sup>-3</sup>	1.940x10 <sup>-3</sup>
1 g/cm <sup>3</sup>	= 10 <sup>3</sup>	1	1.940
1 slug/ft <sup>3</sup>	= 5.154x10 <sup>2</sup>	5.154x10 <sup>-1</sup>	1

### Force

	<u>N</u>	<u>Kgf</u>	<u>dyne</u>	<u>lbf</u>
1 N	= 1	1.020x10 <sup>-1</sup>	10 <sup>5</sup>	2.248x10 <sup>-1</sup>
1 Kgf (Kp)	= 9.807	1	9.807x10 <sup>5</sup>	2.205
1 dyne	= 10 <sup>-5</sup>	1.020x10 <sup>-6</sup>	1	2.248x10 <sup>-6</sup>
1 lbf	= 4.448	4.536x10 <sup>-1</sup>	4.448x10 <sup>5</sup>	1



Canada